Study on Key Factors of Roadway Roof Stability Control

Author: Penghui Wei

Supervisor: Professor Hongtao Liu

„I declare in lieu of oath that this thesis is entirely my own work except where otherwise indicated. The presence of quoted or paraphrased material has been clearly signaled and all sources have been referred. The thesis has not been submitted for a degree at any other institution and has not been published yet."

1 Abstract

Aiming at studying the key factors of roof stability of double-side mining roadway in the superposition stress area in hecaogou coal mine，comprehensive research methods such as field measurement, numerical simulation, laboratory experiment and theoretical analysis were used, the key factors which are "key stratum", "key position" and "key location" were obtained. Based on the core factors affecting the stability of the roadway, this paper also proposes a targeted support scheme, which effectively controls the malignant expansion of the plastic zone and maintains the stability of the roadway. The results show that there are four kinds of aluminum-clay mudstone enrichment areas in the roof of the roadway. Moreover, after detailed analysis of the distribution location of the weak interlayer, it is found that the interlayer mainly exists at the position of 0-3m above the roadway, and the range of roof 0~3m is the "key stratum" controlled by the roof of the roadway. During the transition period from the influence of unilateral mining to the influence of bilateral mining, the plastic zone gradually expanded from the two corners of the roof, and the two corners of the roof were the "key position" to control the malignant expansion of the plastic zone in the roadway. From the law of axial development of the plastic zone along the roadway, the "key location" which controls the stability of the roadway surrounding rock is obtained. A spatial trinity key control technology system is put forward, and a control scheme is given. The control effect is good, which effectively prevents the slagging of the large concrete from hurting people and eliminates the hidden danger of the roof.

Keywords: Double-sided mining, stability, plastic zone

Table of Contents

1 Introduction

1.1 Background of this research

Coal has always been a significant position in China's energy consumption structure, and the coal industry is an indispensable part of the national economy. Coal is always the main body in China's energy consumption structure. It is predicted that coal demand in the middle of 2020 is about 60% of disposable energy consumption. However, because of the non-renewable nature of fossil energy, how to rationally develop and utilize coal resources, it is of great significance to reduce the safety of coal mine safety accidents and to promote the safe and efficient production of coal mine and promote economic development.

Based on Hecaogou coal mine as the research object, the NO. 5 coal seam is the main working bed of grass ditch field, which is buried deeply about 300 m. W The length of the West wing roadway is 2470m, and there are working faces for mining at the same time on both sides. Different from the usual belt type mining, the advance direction of the two working faces is parallel to the west wing roadway. In addition, the two working faces advance in opposite directions and will be mined to the same location at about 1150m west Wing Main lane, as shown in figure 1.1.
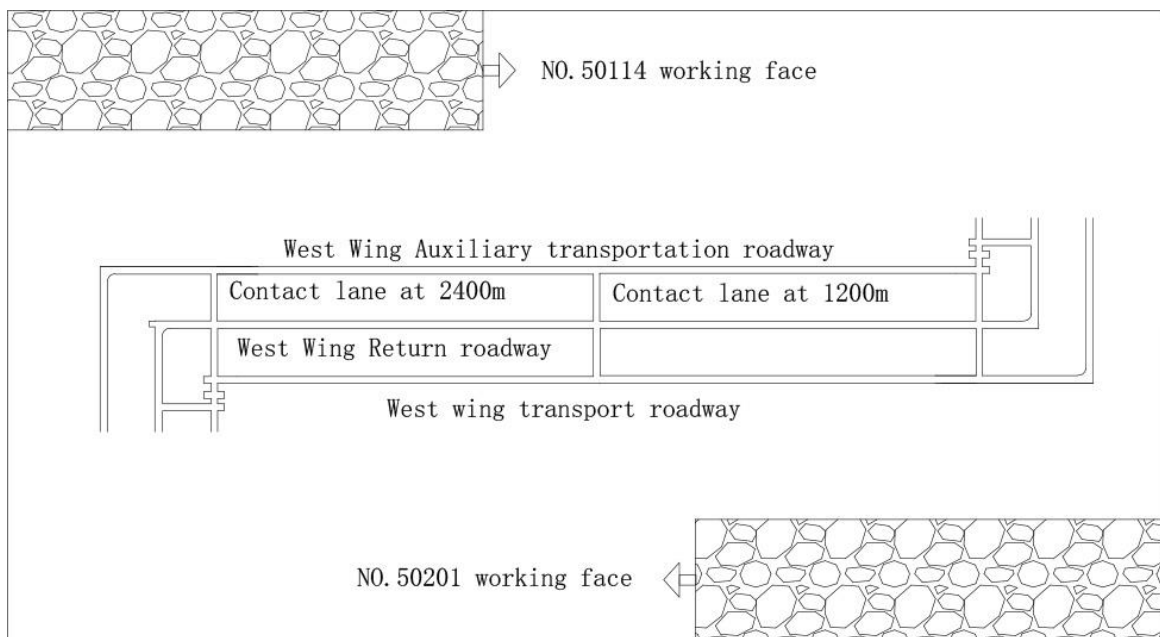

Fig. 1.1 Schematic diagram of mining on both sides of the west wing roadway

The length of 50114 working face and 50201 working face is 260m, and the coal thickness is 2.3m. The length of 50114 working face is 93.3m from the coal pillar of west Wing auxiliary transport roadway, and the length of the channel is 5,200m. The length of the 50201 working face is 100m from the coal pillar of West Wing belt transport roadway, and the length of the channel is 3,200m. At the early stage of mining on the working face, only one side of the roadway was affected by mining, and the roof of the affected roadway was partially filled with concrete slag and bulging.

With the continuous advance of the two working faces, the superposition of mining stress on both sides of the roadway will inevitably occur before and after the intersection of the two working faces of the roadway. This may lead to severe damage to the roof surrounding rock of the roadway, resulting in a large area of concrete slag falling and injuring people, hindering pedestrians in the roadway. More serious may occur failure fracture bolt anchor cable, lead to roof caving of roof accidents. This study is of great significance to prevent slag falling from large concrete roadway on both sides of mining, reduce the maintenance cost of roadway, and ensure safe and efficient mining. At the same time, the study on the stability and control of mining roadway on both sides of other coal mines also plays a certain reference role.

1.2 Research status

1.2.1 Research status of mining stress field distribution

LuJun Wang [1]et al. established a series of strength discriminators to determine the disturbance characteristics of deep coal seams under the influence of mining stress. By means of numerical simulation of deep coal, a numerical simulation model is established to obtain the variation law of stress and the strength characteristics of surrounding rock under the influence of mining. In the research stage, the deformation law of deformation field under the influence of many factors is analyzed, and its rationality is expounded after comparing the measured stress with the simulated result. At the same time, the research results show that under the condition of low coal strength and high rock strength, the deep coal and rock mass will undergo elastic-plastic failure. However, when the mining roadway which is not

affected by the mining of the protective layer is disturbed, its disturbance factor is above 0.7, and the disturbance degree of the coal body will increase with the increase of the disturbance factor.

Shengwei Li et al. studied three types of typical underground mine layout in coal mines, and obtained the stress field of caving coal mining, protective coal mining and column-free mining as well as the distribution of fracture field through UDEC simulation.Research results show that under the influence of different mining fissure morphological differences, but the main characteristics are given priority to with trapezoid, triangle, and tower type. Main column type PCM, TCM major corresponding triangles, and NM basically corresponding to the acme, in the three fracture field, through contrast experiment found that highlight the danger coefficient of large mines, PCM for the gas control effect better [2].

Shujing Zhang through numerical simulation, the use of state of software, the mining stress field is studied and the relationship of percussive ground pressure, the study shows that in the affected by the mining process, the occurrence of percussive ground pressure is mainly related to its high stress and high energy production, after a series of tests, to simulate the mining stress field is verified [3].

Yue Sun believes that the distribution law of overburden collapse is affected by working face mining, and the fracture area and corresponding destruction space caused by overburden collapse will have an impact on roof support and mine safety production. After using FLAC3D numerical simulation for calculation, the correlation test of strike and dip profile was established, and the relation between fracture distribution generated by overlying rock migration and spatial failure morphology was established. It is found that under the influence of mining stress, the overburden from instability to collapse can be explained to a certain extent by uniform law. The failure of overburden can be roughly divided into three steps: unstable bending, broken hinge joint and gradual compaction. Compared with the trapezoidal fracture, the development trend of internal fractures can be described by the laws of formation, development, migration and compaction. After the stress evolution law is simulated by FLAC3D numerical simulation, the evolution of stress field can be analyzed and obtained in three steps, namely, the initial stage of excavation (the roof does not touch the bottom), the middle stage of excavation (the roof touches the bottom) and the later stage of excavation (the overburden compaction touching

the bottom).In the initial stages of the excavation, roof caving stress unloading occur, as the roof caving in contact with the floor, after floor to the roof has played a supporting role, unloading state began to appear gradually slow down trend, which has been transferred upwards of supporting force, which makes the stress gradually stabilized, evolution law of mining stress field also gradually tends to be stable [4].

Ping Zhou et al. took the return ventilation roadway of the 1305 working face of The Guojiahe Coal Mine as the research object. Due to the serious deformation of adjacent roadway during the stopping process, it is necessary to monitor the deformation of surrounding rock and the change of mining stress field during the advance of the working face. Through monitoring and analysis, with the continuous advance of the working face, the deformation velocity of the roadway increased by three to five times compared with that before. As for the unilateral abutment pressure of the return air roadway, its peak value and the extension distance at the coal side were reduced. The large deformation of the return air roadway is affected by the superposition of multiple factors, including mining stress, goaf lateral abatement pressure, lateral roof structure, etc. [5].

Taking Zhuxianzhuang Coal mine as the research object, Qinjie Liu et al. optimized and analyzed the in-situ stress field of the mine by means of the reverse analysis method and obtained the optimal solution of boundary load and the distribution of in-situ stress in this area through the field measurement of local in-situ stress.At the same time, a FLAC3D numerical simulation model was established to study the influence law of mining stress field in the face of work under the influence of factors such as the non-uniformity coefficient of horizontal stress, the Angle between the maximum principal stress and the advance direction, and the lateral pressure coefficient [6].

Hongwei Wang et al. used a similar simulation method to simulate the characteristics of the stress field distribution with the advance of the working face when there are two sets of faults. Through the study found that as the working face mining, a significant rise in stress around the first fault, this is because the line into the ground within the rock mass in the process of gathering a large deformation energy, and with the mining of coal seam, most of this part of the pressure will be transferred to the first fault encountered in the process of mining, it also makes the no.1 fault by stress is greater than the number two fault. But due to the fault to bear

the huge stress, in the event of a sliding phenomenon, after the no. 1 fault affected by dynamic pressure occur first instability phenomenon, that at this point in the overburden deformation energy will be released, the stress of the no.1 DuanCengChu see big changes, while 2 fault stress change relatively smaller number one fault [7].

Pengfei Jiang et al. focused on the study of Majialiang mine, and took the No.4 extra-thick coal seam of the mine as the research object. After numerical simulation and field measurement, the evolution law of the stress field in the stopping process of the stopping roadway in the working face was analyzed. According to Jiang Pengfei et al., the comprehensive stress field not only includes the stress field of the original rock, but also includes the mining stress field and the support stress field generated in the mining process of the working face. After analyzing each stress field one by one, it is found that the original rock stress value above the coal seam roof of this mine is too high, which can be classified as high stress. At the same time, after studying the value and direction of the original rock stress, it is concluded that the mining stress of the roadway rises sharply within 50m of the hysteresis working surface, and gradually tends to be stable after 150m of hysteresis. After the analysis of the supporting stress, under the influence of the pillar support, the rising trend of the supporting stress slightly lags behind the mining stress, and the stability of the stress state depends on the prestress of the anchor cable. The higher the prestress is, the more stable the stress state is. When the prestress of anchor cable is low, its supporting stress will change dramatically [8].

On the basis of numerical simulation and field test, Jianwei Li et al. obtained the distribution of stress field and the characteristics of overlying strata pressure in gully shallow buried coal seam of Chuanchougedan mine through analysis and study. After comparing the ratio of dead weight stress and vertical stress, it is found that due to the influence of the stress field of the original rock, the maximum vertical stress can be determined by the position of this ratio in the coal seam[9].

Jie Liu et al. took Pingmei No. 2 mine as the research object and made a systematic study on the stress distribution of working face direction and tendency direction under the influence of mining action. After monitoring the deep stress field, they obtained the rule of stress change and discussed the dynamic disaster caused by the stress change. The results show that the peak stress is mainly concentrated in

the coal side and a distance under the influence of advanced mining in the working face. At the same time, the stress concentration coefficient is relatively large in these positions, and the stress distribution law is also different.When the peak and gradient of mining stress are analyzed, the characteristics and range that affect the stability of coal seam can be obtained [10].

Meng Lin Xu et al. studied a typical Coal mine S2S9 working face and used three-dimensional numerical simulation to reveal the vertical characteristics of the stress field and displacement field on the surface.The study shows that the overburden migration has a specific rule in thick coal mining.This study can provide reference for safe and efficient mining of other soft overburden in ultra-thick coal seam mining technology [11].

Zhao Qifeng and others by FLAC3D numerical simulation, simulate the stress field distribution characteristics of rock mass under different depth, as well as the characteristics of the displacement field under different depths, obtained in the process of mining, through numerical simulation under the influence of mining stress, coal floor place where the most prone to breakage and under the condition of that the maximum damage depth of [12].

Zhen Wang studied the distribution of roadway stress under the influence of mining and used numerical simulation method to simulate the different stress environment of roadway, so as to analyze the influence of stress on dynamic disaster. After a series of studies, it is found that stress-dominated dynamic disasters usually occur in mine stope, while gas-dominated dynamic disasters tend to occur in roadway [13].

Penghai Zhang et al. studied the underground formed by mining factors in Line 15 of Shrengou mine and analyzed in detail the generation and evolution law of micro-fracture in surrounding rock during this process. Through the establishment of ANSYS mechanics model, the stress distribution law of surrounding rock under the influence of mining is analyzed in detail. The study shows that the occurrence of micro-fracture in surrounding rock is related to the stress state in this area, and the concentration of stress will make the micro-fracture in this area relatively more intensive. In combination with the rock mass condition in this region, it is found that the more concentrated the internal microfractures are, the more serious the internal rock mass failure is. This is because the energy released during the microseismic

activities plays a crucial role in the rock mass failure, which can be used as an index to evaluate the stability of rock mass [14].

Mingzhong Gao et al. obtained the stress evolution law of advanced working face by analyzing the stress of advanced mining and a series of analysis and research on the 8309 working face of Tongxin Mine. The results show that, under the influence of mining factors, abutment pressure rises gradually and increases from the original stress state to the peak strength. Subsequently, with the influence of mining, abutment pressure decreases gradually due to the deepening of coal damage, and finally reaches the residual strength. At the same time, the lateral horizontal stress is different from the leading stress, showing a trend of gradual decrease. According to the division of the distribution area of abatement pressure, it can be divided into four categories: the severe disturbance area in the front of the working face, the strong disturbance area in the range of 50m to 100m, the weak disturbance area in the range of 100m to 200m and above 200m [15].

There are problems in surrounding rock control of non-regular fully mechanized face of inclined coal seam. This study investigates the evolution of mining stress on a varied-length working face at different coal seam dip angles using FLAC3D software to build an experimental model based on the occurrence conditions of inclined coal seams and the layout of a fully mechanized caving working face in western China. Based on the analysis of simulated data, the stress evolution of working face under different dip angles is determined, and the relationship between mining stress evolution and coal seam dip Angle is revealed. The comparison and analysis of the formation and evolution of mining pressure before and after tunnel connection is used to determine the mechanism behind the evolution of mining stress in the short-face and long-face connection process, revealing the difference in the evolution of asymmetric mining stress. Coal seams in the middle and lower reaches of the region are inclined. According to the relationship between the support and surrounding rock, the paper puts forward the structure form of hydraulic support, tunnel layout and supporting characteristics, as well as the control methods to ensure the stability of surrounding rock, such as setting metal mesh above the support and strengthening at the connection of the support. These measures effectively prevent local roof caving and fin spalling, prevent bracket instability and stress concentration at tunnel

connection, and realize safe and efficient mining of irregular working face of thick inclined coal seam [16].

Through FLAC3D, Zhiqiang Sun conducted a series of analysis on the stress of overburden affected by mining, obtained the law of deterioration of the stress, and obtained its distribution form and range by simulating the stress in plastic zone and horizontal section. Studies show that the overlying surrounding rock fissure zone under the influence of mining has typical O-X characteristics of direct roof failure. By studying the failure of plastic zone, it is found that the failure zone presents a saddle distribution pattern with two wing heights and a middle bottom [17].

1.2.2 Research status of surrounding rock stability of roadway

Three-dimensional stress model tests conducted by Daniel Pawelus at copper mines in Poland confirm the existence of high levels of stress in the Lenica-Grox copper Belt (LGCB).No procedure (standard) has been established for the correct selection of stope supports for stope located in areas of high horizontal stress. This is why, for a long time now, as mining engineering progresses deeper into the area of rock, there is a need to identify problems and define standards (procedures) to ensure long-term mining and safe operation of the title, particularly driven by adverse geological and mining conditions. These procedures should include, inter alia, values and directions for high levels of stress. The problems of roadway stability and preparation roadway stability under high horizontal stress in Polish copper mine are studied. The stope stability of Polkowice-Sieroszowice copper mine was evaluated by finite element method. On the basis of Hoek-Brown classification, the rock parameters required for numerical simulation are determined. A RocLab 1.0 computer application was used for this purpose. The stress field parameters were determined based on the underground test of polkowice-Sieroszowice copper mine in 2012.The numerical simulation of Phase2 v. 8.0 in triaxial stress state and plane strain state was carried out. Mohr-coulomb failure criterion is applied to numerical analysis. The softening elastic-plastic model is used to describe the rock medium. The results of numerical analysis provide an application example for bolt support in roadway with high horizontal stress field [18].

By integrating numerical simulation and theoretical analysis, Yuan Fang et al. obtained the distribution of plastic zone, stress and displacement field in the middle

roadway affected by mining. The research results show that the width of the protective coal pillar is inversely proportional to the abutment pressure of the rock around the middle roadway, and the included Angle formed along the goaf roadway and the middle roadway also has a certain influence on the abutment pressure [19].

Through theoretical analysis and statistical regression analysis, and combined with FLAC3D software simulation, Liu Yongli judged the stability relationship between the roadway and the silt-bearing structure layer through the plastic zone of the middle surrounding rock. Through simulation, the stability index of surrounding rocks at different distances is also obtained, which ACTS as the standard of safe distance [20].

Taking Jisan Mine as the research object, Li Xiaoyu et al. simulated the variation of surrounding rock stress of belt conveyor tunneling along the bottom under different sections by FLAC3D.Through the analysis of rectangular section and isosceles trapezoidal section, the evolution law of vertical and horizontal stress of surrounding rock is obtained. The study found that the horizontal displacement of trapezoidal roadway was small, but the vertical displacement was large, and floor heave was more likely to occur [21].

Dai Changchun et al. studied the distribution of surrounding rock stress and its failure law of coal roadway under coal mining in the upper coal seam during mining by using FLAC3D numerical simulation, taking transportation roadway at working face 05 of Jisan Mine as the research object. Through the study, it is found that the effect of anchor cable support is limited. Under the action of horizontal stress, the surrounding rock deformation of roadway is large, and the horizontal stress has a significant influence on the stability of roadway [22].

Zhao Zhiqiang studied the deformation and failure essence of large deformation mining roadway in Baode mine. After sufficient theoretical analysis, laboratory experiment, numerical simulation and field test, the failure law and degree of surrounding rock of large deformation stopping roadway are determined to a certain extent by the geometry of plastic zone. It is found that by deducing the boundary equation of the plastic zone of circular roadway, the "butterfly shaped" plastic zone is formed under the influence of various factors such as stress and lithologic combination of roadway section. The relationship between the plastic zone shape of surrounding rock and the shape variables of surrounding rock is obtained with the

influence of mining on the working face. On this basis, the relationship among support, plastic zone and surrounding rock deformation is established, and the roadway is mainly affected by the superposition stress field. In order to prevent malignant expansion of plastic zone boundary caused by such deformation, the technology of co-support between elongable bolt and ordinary bolt is proposed. Field engineering tests also show that this technology can provide stable support resistance for roadway and effectively prevent malignant expansion of plastic zone [23-24].

He Fulian et al. solved the problem that it is difficult to control the surrounding rock stability of deep soft rock roadway by studying the underground car yard of Xingdong Mine. Through a series of numerical simulation, field observation and experiment, the failure mechanism of deep soft rock under high stress environment is explored, and the stress field and displacement field of surrounding rock are studied according to its failure form and failure law. After to express the combined support system, to support site monitoring, obtained the bearing capacity of anchor and shotcrete layer as a function of anchor spacing, power exponent function trend growth, and the bearing capacity of the spray layer thickness and its structure is present a linear growth, but at the same time when the thickness of 200 mm, sharply reduce tensile stress area[25].

Zhang Zhaoqian et al. selected a variety of factors to evaluate the stability of surrounding rocks, and determined their impact factors according to the impact of each factor on the stability of surrounding rocks, and determined the weight of each impact factor through analytic hierarchy process. After a series of studies, the calculation model and calculation method of a single comprehensive index were established to scientifically reflect the stability characteristics of roadway surrounding rocks [26].

1.2.3 Research status of roadway support technology

Huang Qingxiang et al. studied the self-equilibrium phenomenon of surrounding rock collapse backwardness and believed that self-stable equilibrium arch existed in roadway surrounding rock collapse backwardness. According to the principle of tensile failure and non-tensile stress conditions, the elliptic curve equation describing the ultimate self-stable equilibrium arch could be obtained. This

theoretical equation describes the properties of the interaction between the bottom plate, the roadway top and the roof, and proposes that the support should be matched with the corresponding self-stabilized balance ring [27].

Based on zhaolou Coal Mine, Li Weiteng et al. proved the feasibility and effectiveness of the new type support by studying the high-stress soft rock roadway. Through FLAC3D experiment, the support system of arch frame in roadway was simulated. By dividing the influencing factors into support strength, surrounding rock strength and in-situ stress level, the influencing laws of these factors on the shape variables of roadway surrounding rock, the scope of producing plastic zone and the stress state of supporting members in arch support system are analyzed and discussed. Research shows that arch support has certain stiffness and corresponding strength, which can effectively control surrounding rock deformation [28].

Kang Hongpu et al. studied the action mechanism of anchor bolt on supporting and emphasized the action effect of anchor bolt prestress and prestress diffusion. Especially when supporting roadway with complex surrounding rock environment, the deformation and failure of surrounding rock should be effectively controlled as soon as possible. The study also introduces some complete set of bolt support technologies, including high-strength bolt and anchor cable support materials, roadway surrounding rock geomechanical testing technology, anchoring and grouting combined reinforcement technology, etc. [29-31].

Through FLAC3D, Wang Jinhua simulated the roadway in Datang Tashan Coal Mine and studied the stress and deformation of surrounding rock by means of multi-factor comprehensive comparison. It is found that the stress and deformation of surrounding rock show different characteristics under different top coal thickness, tunnel position, aspect ratio, ground stress and anchor cable preload. When the thickness of top coal is less than 10m, the stress concentration area of driving roadway in coal pillar is distributed by triangle. The wider the roadway is, the more concentrated the stress in the top coal, and the higher the strength of coal and rock is, the greater the stress value of surrounding rock will be. When combined support of bolt and cable is used, the pretension in bolt and cable will present stress zones superimposed on each other, which can effectively control the deformation of surrounding rock [32].

By integrating rock mechanics experiment, numerical simulation and theoretical analysis, And taking Huinan mining area as the research object, Yuan Liang et al. explored the standard system of surrounding rock classification of deep rock roadway. Under the coupling effect of three high levels, four theoretical principles for controlling the stability of deep surrounding rocks were proposed, and the complete set of technologies for controlling the stability of surrounding rocks in Huainan mining area were summarized [33].

Taking Xinwen Mine as the research object, Kang Hongpu et al. focused on the problem of roadway support under a kilometer deep well. By analyzing the stress environment and surrounding rock environment of deep roadway, UDEC numerical simulation was used to study the supporting effect of different supporting methods and parameters on the deformation and failure of surrounding rock of deep roadway. The study shows that the super-kilometer deep well of Xinwen Mine is more suitable for the combined support mode of high prestress, high strength bolt cable and grouting, which is helpful to ensure the long-term stability of surrounding rock [34].

Liu Hongtao et al. developed a new type of extendable bolt which can be used to control the deformation of surrounding rock in large deformation roadway. This study takes Wujiagou coal mine as the research object. By constructing constitutive model of surrounding rock support system, the stress and deformation characteristics of traditional bolt and elongated bolt are compared and analyzed. The results show that the maximum extension of the connecting bolt with a length of 4m can reach 685mm.Through the adoption of extendable bolt, the subsidence of the roof is reduced by more than one third, realizing strong support and effective pressure relief [35].

1.3 Main research content of this thesis

The main contents of this thesis are as follows:

(1) By studying the distribution of roadway roof strata, the distribution of weak interlayer and the development of fractures in roadway roof strata were obtained by using borehole peeping technique. Through the analysis of the weak interlayer and fracture zone, the key strata that affect the stability of roadway under the influence of bilateral mining are determined.

(2) Study on the development law and stability of roadway ore pressure affected by mining. FLAC3D numerical simulation was used to analyze the stress field and superposition influence of roadway surrounding rocks during tunneling, under the influence of unilateral mining and under the influence of both sides of mining. The distribution law of deformation and plastic zone of roadway surrounding rock was studied, the failure mechanism of roadway surrounding rock with bilateral mining was revealed, and the key position and key location of stability of roadway surrounding rock affected by mining were obtained.

(3) The key control technology and scheme of surrounding rock stability of roadway affected by mining were studied. According to the key factors that influence the stability of roadway obtained by the research, the key techniques and schemes for controlling the stability of surrounding rock are put forward. And through the industrial test, verify whether the key point of the roadway can be controlled to ensure the stability of the roadway.

2 The key layer stability of roadway roof strata

2.1 Visual detection of roadway roof strata

2.1.1 Peep scheme design of west wing roadway roof

In order to obtain the result of borehole peeping with high precision, the ZKXG30 mine borehole imaging trajectory detection device is selected as the peeping instrument of the west Wing roadway roof, which can carry out omni-directional imaging of the borehole. The experimental instrument can take pictures, record video and measure the trajectory of the borehole to ensure the smooth completion of the experiment. By peering into the borehole, the high-definition dynamic video inside the borehole can be obtained, and high-resolution photos can be taken locally to obtain the layout of the full hole wall expansion and the spatial track of the borehole, as shown in Figure 2.1.

Fig. 2.1 ZKXG30 mine based safe borehole trackmeter

Since the length of the roadway exceeds 2400m, when setting the peeping point position of borehole, the representative peeping point position of 2400m, 1240m and 410m should be set. Borehole peeping tests were conducted on the roof and return air roadway of west Wing return air roadway, auxiliary transport roadway, and west wing belt transport roadway. The roof has 7 holes, and the layout of borehole peeping points is shown in Figure 2.2.
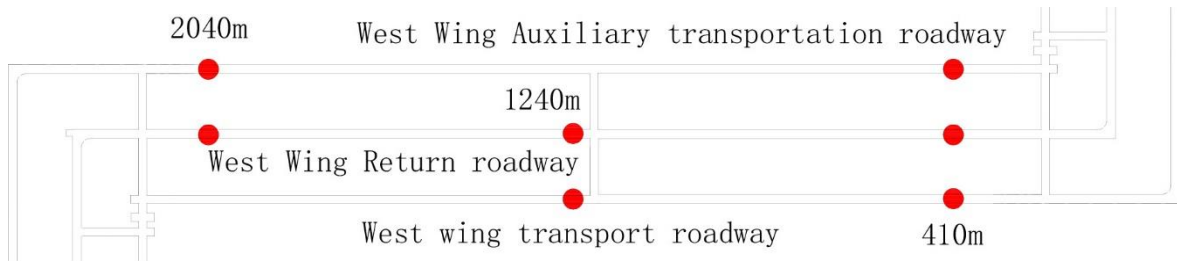
Fig. 2.2 Arrangement of borehole observation points

Drilling is divided into roof drilling and roadway drilling. There are two types of roof borehole, 8m borehole and 13m borehole, and two meters of borehole are taken from the roadway side. The borehole at the side of the roadway is only at 1240m of the return air main roadway in the west wing, and the detailed distribution of the rest roof peeping points is shown in Table 2.1：

Tab.2.1 Distribution table of roof drilling in west wing roadway

	2040m		1240m		410m	
	8m borehole	13m borehole	8m borehole	13m borehole	8m borehole	13m borehole
Auxiliary roadway	√				√	
Return air roadway	√			√	√	
transport roadway			√		√	

Due to the large number of data, the representative roof peek-hole at 2400m, 1240m and 410m of the west wing return air lane is taken for sampling statistics and detailed analysis, so as to obtain the distribution of unstable rock strata.

2.1.2 Analysis of borehole peep results of West wing roadway

After drilling the surrounding rock, the peeping instrument was used to peer into the surrounding rock of the roadway. The obtained peeping conclusions of the west wing return wind roadway are shown as follows. Through the detailed analysis of borehole peep map, we can get more detailed distribution of rock strata. In particular, the distribution of extremely thin rock strata of aluminous mudstone, the interbedding distribution of aluminous mudstone and other rock strata, and the distribution and development of fractures in overlying strata of

roadway can be obtained, which will provide the most detailed data support for further research in the later stage.

(1) Borehole peep at the 410m roof of the west Wing Return Wind Roadway

By analyzing the peeking video of the roof borehole at 410m of the West wing return air roadway, the distribution of rock strata at 410m of the return air roadway can be obtained. A typical peeping borehole map is taken here, and its screenshot is shown in Figure 2.3:
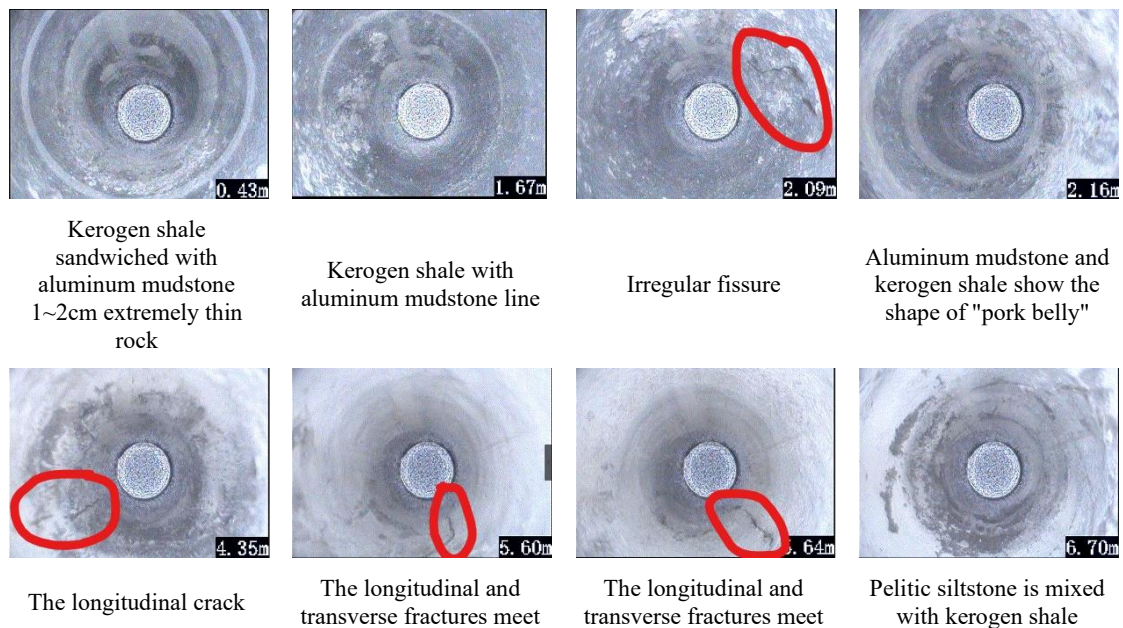

| Kerogen shale sandwiched with aluminum mudstone 1~2cm extremely thin rock | Kerogen shale with aluminum mudstone line | Irregular fissure | Aluminum mudstone and kerogen shale show the shape of "pork belly" |
| The longitudinal crack | The longitudinal and transverse fractures meet | The longitudinal and transverse fractures meet | Pelitic siltstone is mixed with kerogen shale |

Fig. 2.3 Peep view of 410m roof borehole in the backwind roadway in the west wing

It can be seen from the peeping borehole results of the 410m roof of the Return wind roadway in The West wing that the kerogen shale is interbedded with aluminum mudstone thin layer within the range of 0~3.6m, and the extremely thin layer of aluminum mudstone appears at 0.2m, 0.45m, 0.5m, 0.63m and 0.8m.At 0.9m, 1.15m and 1.95m, a 10cm aluminous mudstone thin layer appeared.There are three aluminum mudstone lines of 0.5~1cm at 1.15m ~1.75m.From 2.05 m to 2.45m, 2 sections of aluminum mudstone and kerogen shale interbedded in the form of "pork belly".In addition, irregular fractures appeared at 2.1m, and 5 extremely thin layers of aluminous mudstone (1~2cm) appeared at 2.82-3.0m.

lithology	Tired of deep/m	layer thickness /m	Rock column diagram
argillaceous siltstone	8.0	4.4	
kerogen shale	3.6	3.6	

Fig. 2.4 Histogram of roof rock structure of 410m in the backwind roadway in the west wing

In the range of 3.6~8m, it is mainly argillaceous siltstone. In some areas, argillaceous siltstone is interbedded with thin layers of kerogen shale.The "streaky" interbedded state of argillaceous siltstone and aluminous mudstone appears between 4.20m and 4.50m.Longitudinal fractures appeared at 4.35m, 5.6m and 6.4m, and the rock layer was basically intact without fracture.The mixture of argillaceous siltstone and kerogen shale at 6.5~6.8m is interbedded with no rock fragmentation and is basically complete.The distribution of the overburden of the roof at 410m obtained by detailed analysis of the rock strata is shown in FIG. 2.4

(2) Peeping through the 1240m roof borehole of the Return Air Lane in the West wing

By analyzing the peeping video of the roof borehole at 1240m of the West wing return air roadway, the distribution of rock strata at 1240m of the return air

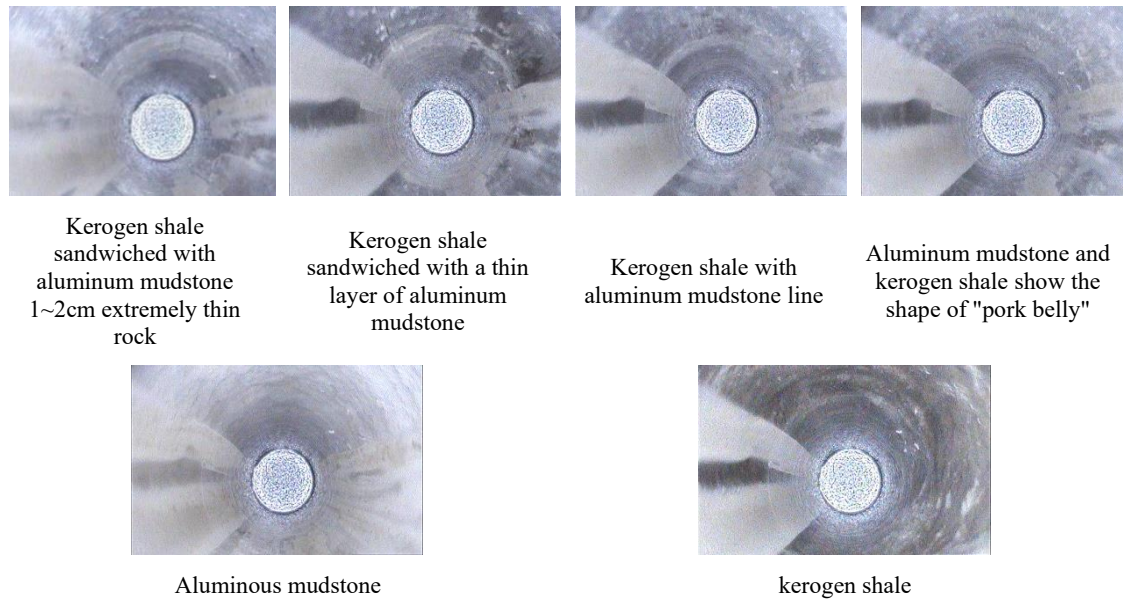roadway can be obtained.A typical peeping borehole map is taken here, and its screenshot is shown in Figure 2.5:

Kerogen shale sandwiched with aluminum mudstone 1~2cm extremely thin rock

Kerogen shale sandwiched with a thin layer of aluminum mudstone

Kerogen shale with aluminum mudstone line

Aluminum mudstone and kerogen shale show the shape of "pork belly"

Aluminous mudstone

kerogen shale

Fig. 2.5 Roof borehole peeping diagram of 1240m backwind lane in the west wing

It can be seen from the peeping borehole results of the roof of the 1240m roadway in West Wing that the kerogen shale is interbedded with aluminum mudstone within the range of 0~5.1m, and the kerogen shale and the aluminum mudstone are interbedded in the form of "pork belly" in some areas.Three extremely thin layers of aluminous mudstone (1~2cm) appear continuously at 0.08~0.4m.At 0.5m, 0.8m, 1.1m, 1.3m, 1.5m, 1.6m, about 5~10cm aluminous mudstone thin layer.Four aluminaceous mudstone lines of 0.5~1cm appeared continuously at 1.62~1.8m.The kerogen shale and aluminous mudstone at 2.4-2.8m are in the shape of "pork belly".At 3.76m and 3.84m, extremely thin layers of aluminum mudstone (1~2cm) appear. On the whole, the rock strata are basically complete without breakage.

Within the range of 5.1~10.2m, the thin layers of argillaceous siltstone kerogen shale are interbedded in some regions. The aluminous mudstone and argillaceous siltstone appeared at 5.65~5.85m in the interbedded state of "streaky flesh". At 8.15m, 8.8m and 9.05m, the thin layers of kerogen shale with a thickness of 15cm ~20cm appear intact.The lithology is argillaceous siltstone in the range of 10.2~13m.

lithology	Tired of deep/m	layer thickness /m	Rock column diagram
argillaceous siltstone	13	7.9	
kerogen shale	5.1	5.1	

Fig. 2.6 Column diagram of roof rock structure of 1240m in the backwind roadway in the west wing

(3) Peep through borehole of roof 2040m of return air Lane in the West wing

By analyzing the peeping video of the roof borehole at 2040m of the West Wing return air roadway, the rock strata distribution at 2040m of the return air roadway can be obtained. A typical peeping borehole map is taken here, and its screenshot is shown in Figure 2.7:
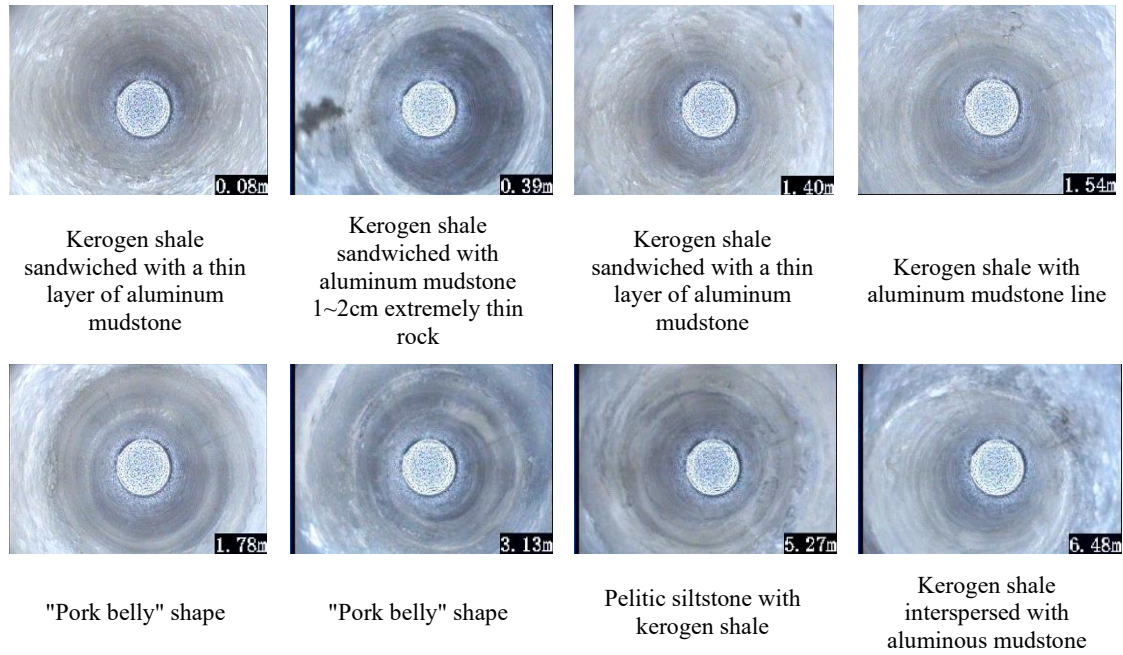
Kerogen shale sandwiched with a thin layer of aluminum mudstone	Kerogen shale sandwiched with aluminum mudstone 1~2cm extremely thin rock	Kerogen shale sandwiched with a thin layer of aluminum mudstone	Kerogen shale with aluminum mudstone line
"Pork belly" shape	"Pork belly" shape	Pelitic siltstone with kerogen shale	Kerogen shale interspersed with aluminous mudstone

Fig. 2.7 Roof borehole observation of 2040m backwind lane in the west wing

lithology	Tired of deep/m	layer thickness /m	Rock column diagram
kerogen shale	8	1.95	
Thin layer of argillaceous siltstone with oil shale	6.05	3.05	
kerogen shale	3	3	

Fig. 2.8 Column diagram of roof rock structure of 2040m in the backwind lane in the west wing

It can be seen from the peeping borehole results of 2040m roof of the return air roadway in the West wing that the kerogen shale is covered with aluminum mudstone thin layer within the range of 0~2.2m.At 0~0.38m, 4-5cm aluminous mud thin layer appeared.Extremely thin rocks of 1~2cm aluminum mudstone appear at 0.40m, 0.56m, 0.69m and 1.22 m.A 2-5cm aluminium-clay thin layer appears at 1.4~1.5m.From 1.54 to 1.6m, four aluminous mudstone lines of 0.5 to 1cm appeared continuously, and longitudinal cracks appeared at 1.54.Between 1.78 and 1.97m, kerogen shale and aluminum mudstone are arranged in the form of "pork belly". The rock layer is basically complete without breakage.

The argillaceous siltstone is interbedded with kerogen shale in the range of 3.2~6.05m.The "streaky flesh" arrangement of kerogen shale and argillaceous siltstone was presented at places 2.62~2.90 and 3.03~3.40.Kerogen shale thin layer 5~10cm long appears at 4m.Two kerogen shale rock lines of 0.5~1cm appeared continuously at 5.27~5.30m.On the whole, the rock stratum is basically not broken, and the rock stratum condition is basically complete.

2.2 Key layer analysis affecting the stability of roadway roof

The distribution of roadway roof strata was obtained more accurately to a certain extent through peeping through the borehole and coring through the borehole.In particular, the distribution of soft interlayer of aluminous mudstone is determined, including the rich area of "belly flesh" in the aluminous mudstone line, the extremely thin layer of 1~2cm of aluminous mudstone, the thin layer of 5~10cm of aluminous mudstone and the interlayer of aluminous mudstone and kerogen shale.The range of unstable strata of roof strata above the main roadway is discussed by analyzing the data from borehole peeping.

(1) Analysis of key unstable rock formations of roof at 2040m of roadway.

According to the above analysis, combined with the distribution of aluminaceous mudstone seen from the previous borehole, after more detailed data processing of the distribution of aluminaceous mudstone, the distribution map of soft interlayer of aluminaceous mudstone as shown in FIG. 2.9 can be

obtained.Through this figure, the distribution of aluminous mudstone in overlying strata of roadway can be more directly reflected.
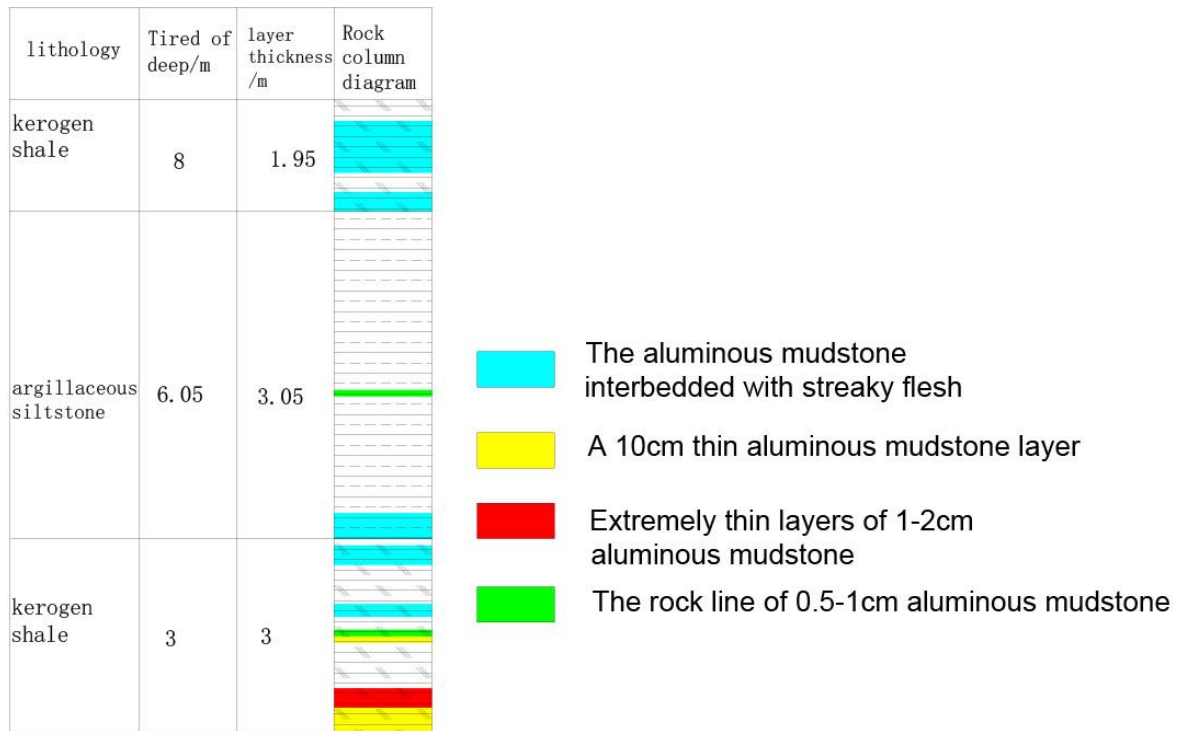
lithology	Tired of deep/m	layer thickness /m	Rock column diagram
kerogen shale	8	1.95	
argillaceous siltstone	6.05	3.05	
kerogen shale	3	3	

The aluminous mudstone interbedded with streaky flesh

A 10cm thin aluminous mudstone layer

Extremely thin layers of 1-2cm aluminous mudstone

The rock line of 0.5-1cm aluminous mudstone

Fig. 2.9 Distribution diagram of weak interlayer at 2040m

It can be seen from the figure that the soft interlayer of aluminous mudstone is mainly distributed within the range of 3m of the roof.This part is mainly dominated by kerogen shale, intermixed with some aluminous mudstone. In the range of 3-6.05m, the rock strata are mainly argillaceous siltstone, and there are a few thin layers of kerogen shale in this layer.The above 6.05m is mainly dominated by kerogen shale, with some aluminum mudstone thin layers interspersed with the rock layer.

(2) Analysis of key unstable rock formations of roof at 1240m of roadway.

According to the above analysis, combined with the distribution of aluminaceous mudstone seen from the previous borehole, after more detailed data processing of the distribution of aluminaceous mudstone, the distribution map of soft interlayer of aluminaceous mudstone as shown in FIG. 2.10 can be

obtained.Through this figure, the distribution of aluminous mudstone in overlying strata of roadway can be more directly reflected.
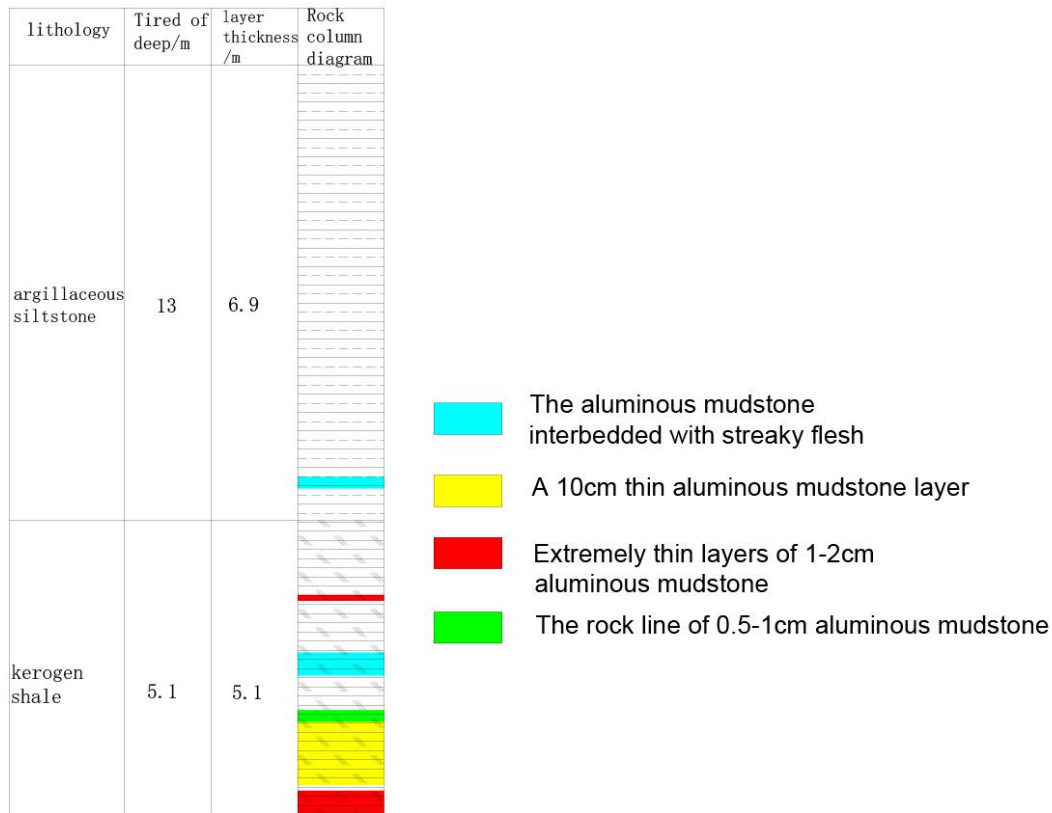

Fig. 2.10 Distribution diagram of weak interlayer at 1240m

It can be seen from the figure that the kerogen shale layer is mainly distributed within the scope of 5.1m of the roof, which is mainly dominated by kerogen shale with some aluminum mudstone mixed in the middle. Above 5.1m, the rock strata are mainly argillaceous siltstone.

(3) Analysis of key unstable rock formations of roof at 410m of roadway.

According to the above analysis, combined with the distribution of aluminaceous mudstone seen from the previous borehole, after more detailed data processing of the distribution of aluminaceous mudstone, the distribution map of soft interlayer of aluminaceous mudstone as shown in FIG. 2.11 can be obtained.Through this figure, the distribution of aluminous mudstone in overlying strata of roadway can be more directly reflected.
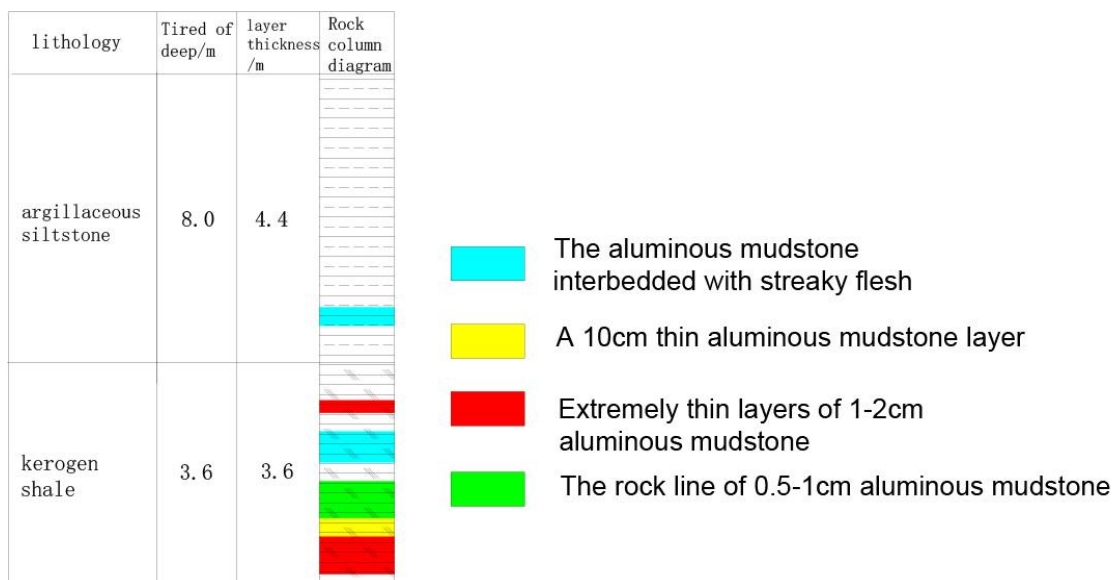
Fig. 2.11distribution diagram of weak intercalations

After obtaining the distribution of soft aluminous mudstone intercalation on the roof of the roadway, combining the rock column map obtained at each location with the roadway location, the bedding distribution of soft aluminous mudstone intercalation along the roadway as shown in FIG. 2.12 can be obtained.
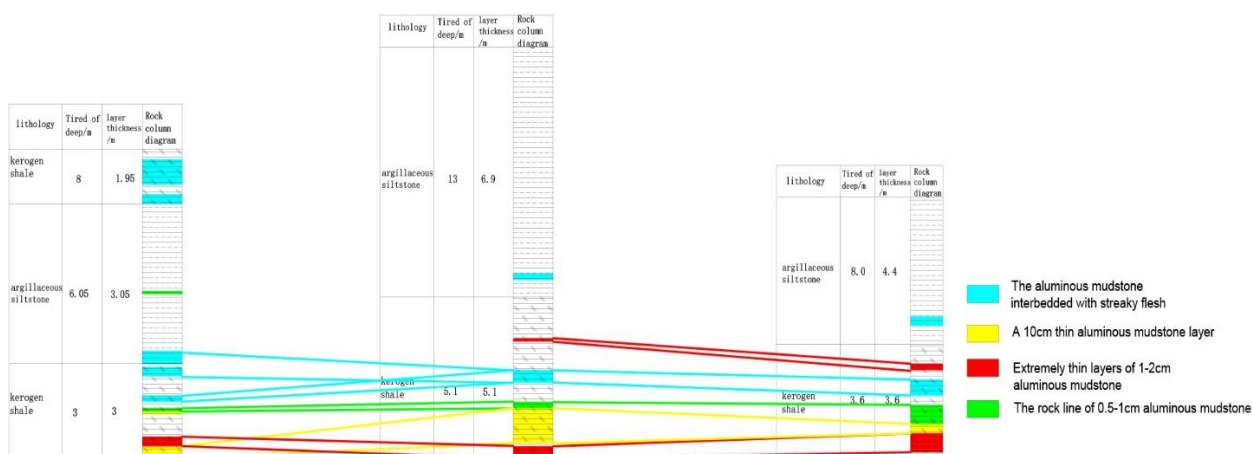

Fig. 2.12 Histogram of intercalation distribution of weak intercalations

It can be seen from the distribution diagram of soft intercalation of aluminous mudstone that the soft intercalation of aluminous mudstone is mainly distributed in the range of 0-3m of roadway roof.Within 3m of the overlying strata of the main roadway, there are dense lines of 0.5-1cm aluminous mudstone, extremely thin layers of 1-2cm aluminous mudstone, thin layers of 10cm aluminous mudstone, and streaky interbedding between aluminous mudstone and other strata.

Aluminous mudstone is easy to be broken by weathering and soften when exposed to water. These properties make the 0-3m rock layer overlying the roadway present an extremely unstable state, affecting the stability of the roadway.Under ideal conditions (without considering the abrupt change of strata), the corresponding aluminous mudstone interlayer interval is connected to obtain the aluminous mudstone interlayer distribution diagram of the overlying strata of the roadway as shown in the figure.

The soft interlayer of aluminum mudstone gradually decreases from 3.4m at 2400m of roadway to 400m of roadway 4.However, the main distribution interval of aluminous mudstone interlayer is within the range of 0-3m in the surrounding rock of the overlying roadway.Therefore, it can be basically determined that the 0-3m range of roadway roof is the unstable horizon of overlying strata.This key layer needs targeted support to ensure the safety of both mining roadway.

3 Evolution law of mining stress and roadway stability

3.1Analysis of surrounding rock stress field and failure law of Roadway

3.1.1 Numerical simulation scheme for surrounding rock stress of Roadway

The three main roadways of Grass ditch mine are straight wall semicircle arch roadways. The simulated roadway size is 5500mm×4350mm in width × height of the West Wing Auxiliary roadway. The width × height of the return air main lane is 5500mm×4150mm.The width × height of the conveyor roadway is 5500mm×4150mm. The length of the three lanes is about 2500m.The specific roadway section is shown in FIG. 3.1.
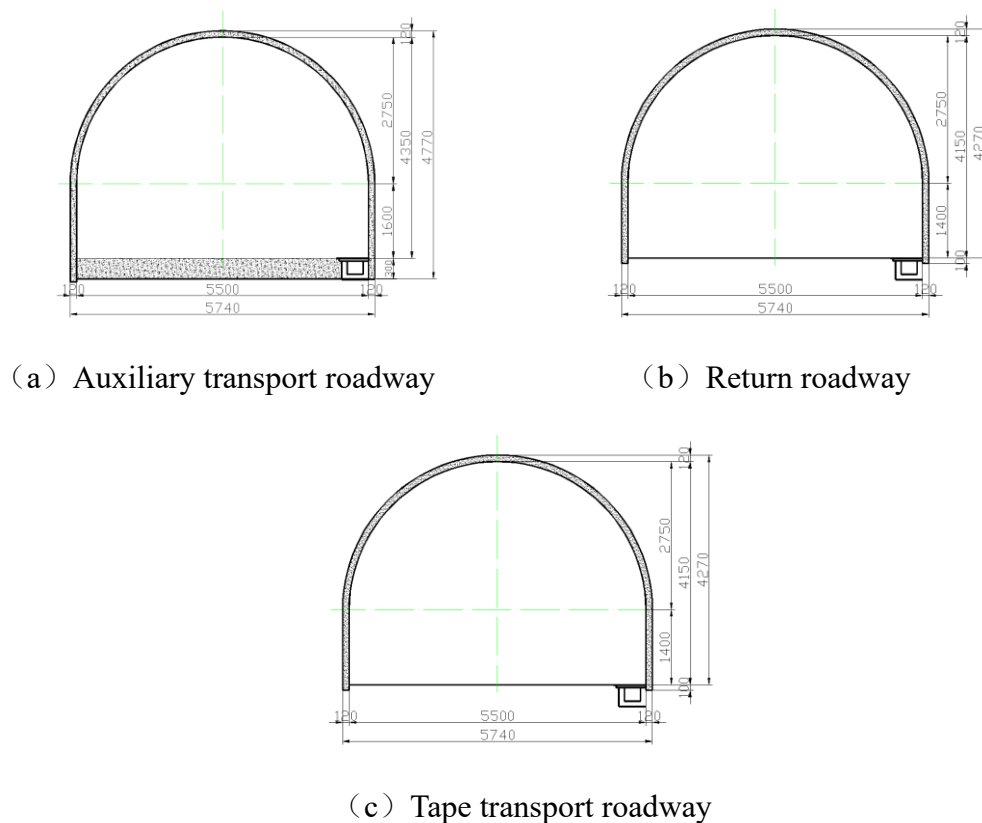
（a）Auxiliary transport roadway   （b）Return roadway

（c）Tape transport roadway

Fig. 3.1 Section diagram of west wing roadway

The No.50114 working face and No.50201 working face are both 260m in length and about 300m in depth, with an average thickness of 2.3m.The width of coal

pillar between the No.50114 stoping face and the auxiliary roadway in the west wing is 93.3m.The width of coal pillar between the working face and the west wing belt conveyance roadway is 100m.The width of coal pillar between the auxiliary roadway of the West wing and the return air roadway of the West wing is 35m.The width of coal pillar between west Wing return air roadway and West Wing belt transport roadway is 35m.
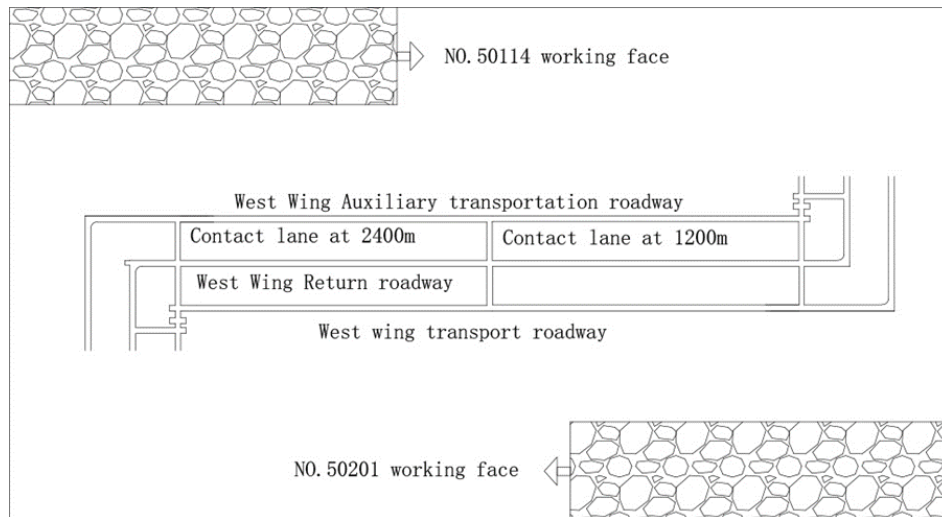

Fig. 3.2 Mining engineering schematic diagram

The roadway drifts along the coal floor. The direct roof of the roadway is mainly oil-bearing shale, while the floor of the roadway is mainly argillaceous siltstone and medium-grained siltstone. The whole model is 160m in height, 919.1m in width and 3700m in length, that is, the size is X*Y*Z=919.1*3700* 160m.The specific mining project is shown in Figure 3.3.The grid at 10m position around the simulated three large roadway was delimited, and the width of the grid in this area was 0.5m. Figure 3.2 shows the actual simulation model. According to the field geological conditions, the vertical stress on the upper boundary of the model is about equal to the dead weight of the rock above it, which is about 6.91mpa, and the lateral pressure coefficient is 1.0.Horizontally, the displacement and initial velocity in the x direction are limited. The base of the model limits the displacement and initial velocity in x, Y and Z directions. The more-Coulomb criterion based on elastic-plastic theory is used in the simulation.
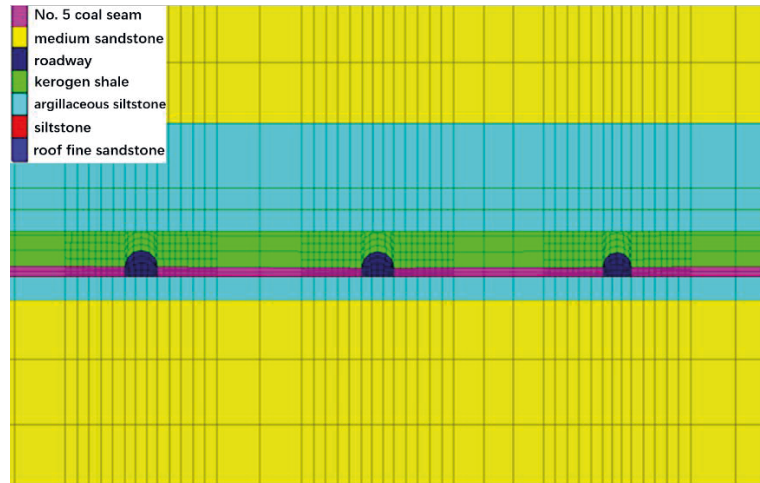
（a）Stratigraphic distribution
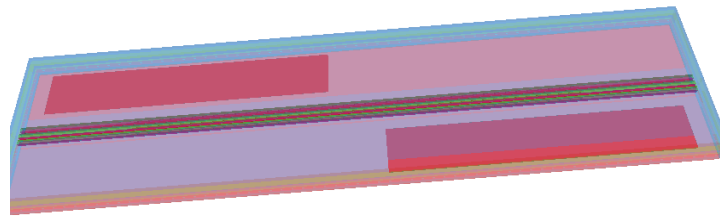
（b）Model perspective

Fig. 3.3 Schematic diagram of numerical simulation model

Mechanical parameters of each rock layer in the model are shown in Table 3.1。

Tab. 3.1 rock mechanics parameters table

stratum	bulk modulus /GPa	tensile strength /MPa	internal friction angle /°	density /kg/m³	cohesion / MPa	thickness /m
siltstone	2.55	3.35	34	2490	6.14	41
medium sandstone	4.4	2.49	37.3	2840	4.04	60
argillaceous siltstone	3.55	1.55	27.7	2490	5.5	11
kerogen shale	2.51	2.20	33.5	2460	10.1	6.1
No. 5 coal seam	8.90	0.94	23.54	1390	2.74	2.3
argillaceous siltstone	3.56	2.10	21.7	2460	2.46	4.2
medium sandstone	2.86	1.59	30.3	2550	1.77	35.4

Numerical simulation was carried out to calculate the stress of three large roadways when two working faces were pushed to different positions. The stress cloud map and plastic zone map are used to analyze the stress of the roadway and the failure of the roadway when the working face is pushed to different positions. According to the actual progress of the site, the 50114 stope face and 50201 stope face will be mined to the same location at 1150m.Five observation stations a, B, C, D and E were established respectively. The observation station E was located at the intersection of the two working faces at 1150m.The observation station A, B, C and D are 300m, 200m, 100m and 50m from the observation station E respectively. After the two working faces are pushed to the position shown in the figure (denoted as push 0m), they continue to push forward at the same time 100m, 200m, 250m, 300m, 350m, 400m, 500m and 600m, and record the distribution of surrounding rock stress and plastic zone at each position. The numerical simulation model is shown in Figure 3.4.
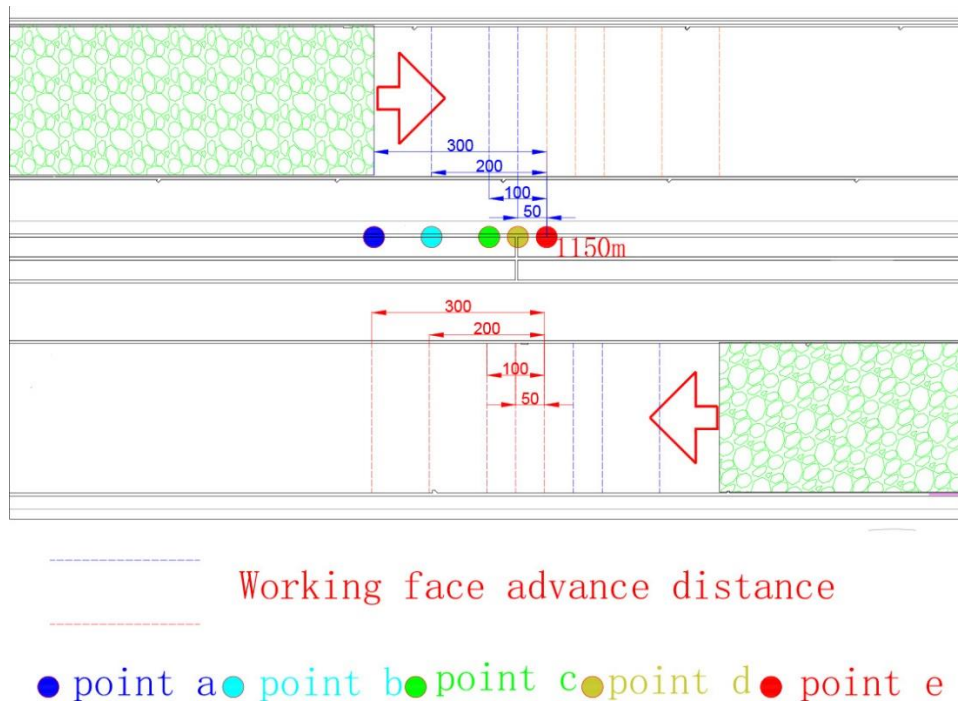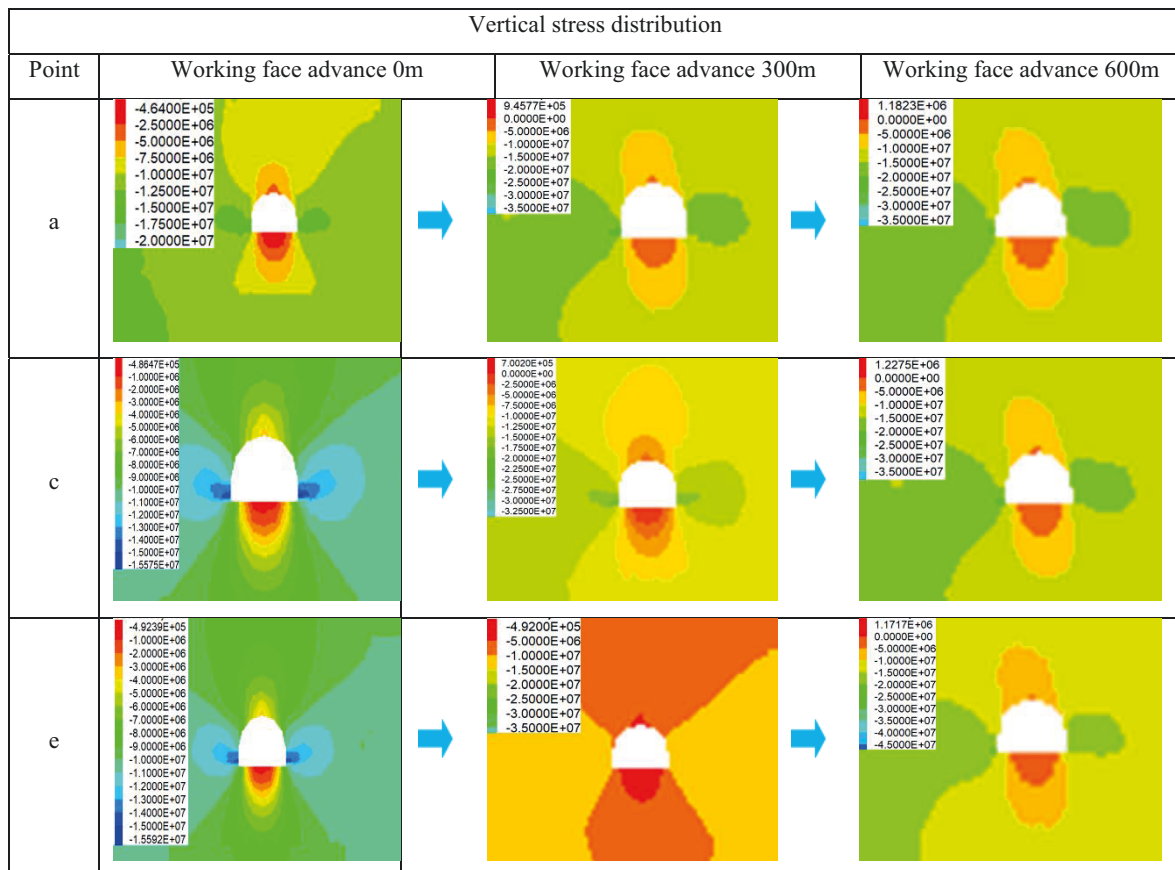

Fig.3.4 Schematic diagram of numerical simulation model

3.1.2 Analysis of the evolution law of the surrounding rock stress field of the two-sided mining roadway

After the working faces on both sides of the roadway are pushed to the position shown in FIG. 3.4, the two working faces continue to push forward the same distance at the same time and advance successively to the position corresponding to the red and blue dotted line in the figure.Record the horizontal and vertical stresses of the main roadway advancing to the observation station A, B, C, D and E in turn.When the working face continued to advance by 300m, the two working faces were advanced to the same position.When the working face is pushed forward by 0m, 300m and 600m, the vertical stress and horizontal stress distribution of station A, C and E are shown in Figure 3.5. The vertical stress is the maximum value at the roadway side, while the horizontal stress is the maximum value at the roof.
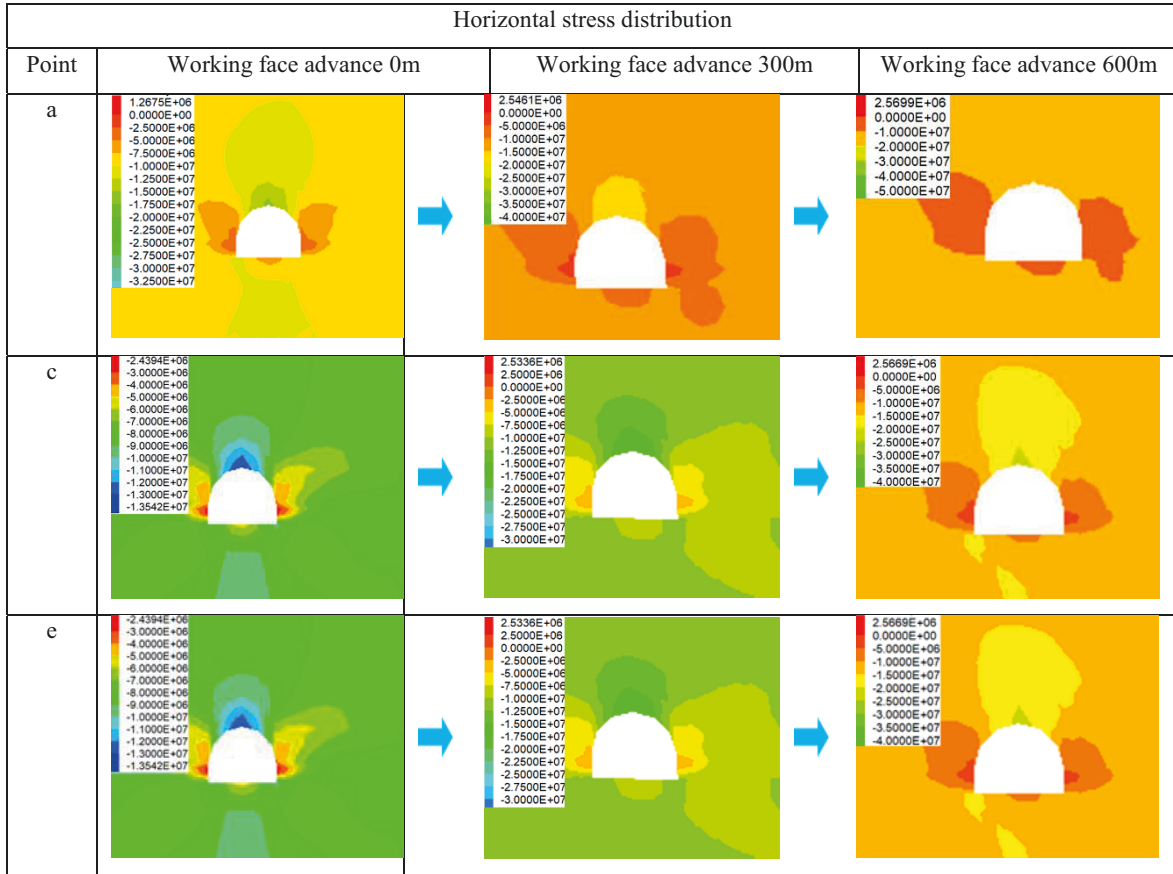
Vertical stress distribution		
Point	Working face advance 0m	Working face advance 300m	Working face advance 600m
a			
c			
e			

Horizontal stress distribution			
Point	Working face advance 0m	Working face advance 300m	Working face advance 600m
a			
c			
e			

Fig.3.5 Horizontal stress and vertical stress distribution

Without engineering disturbance, the vertical stress of the West wing roadway is 9.7mpa.During tunneling, the maximum vertical stress around the roadway was 15MPa, 1.5 times that of the original rock stress. Before the intersection of 50114 working face and 50201 working face, the maximum vertical stress around the roadway was 20MPa during the period when the roadway was only affected by unilateral mining.The stress is located at the two sides of the roadway, and the stress concentration coefficient is 2.1, 1.3 times that of the excavation period. After the intersection of 50114 working face and 50201 working face, the roadway was affected by bilateral mining, and the vertical stress was further increased. The stress affected by unilateral mining increased to 25MPa by 20MP, and the stress concentration coefficient was 2.6, which was 1.7 times that of the tunnelling period. This indicates the superposition of vertical stresses.

Without engineering disturbance, the horizontal stress of the West wing roadway is 7.8mpa.The maximum horizontal stress is 13MPa, which is 1.7 times of the original rock stress.Before the two working faces intersect, the roadway is only

affected by unilateral mining, and the maximum horizontal stress around the roadway is 20MPa.The maximum stress is located at the roof and bottom Angle of the roadway, and the stress concentration coefficient is 2.5, 1.5 times that of the tunneling period.After the intersection of the two working faces, the roadway was affected by bilateral mining, and the horizontal stress around the roadway increased from 20MP in the case of unilateral mining to 30MPa in the case of bilateral mining stress.At this time, the stress concentration coefficient is 3.8 times that of the tunneling period.This indicates the superposition of horizontal stress.

After recording and analyzing the statistical data of each station, taking the statistical data of station e as the sample, the evolution regularity diagram of vertical stress and horizontal stress is drawn, as shown in Figure 3.6.。
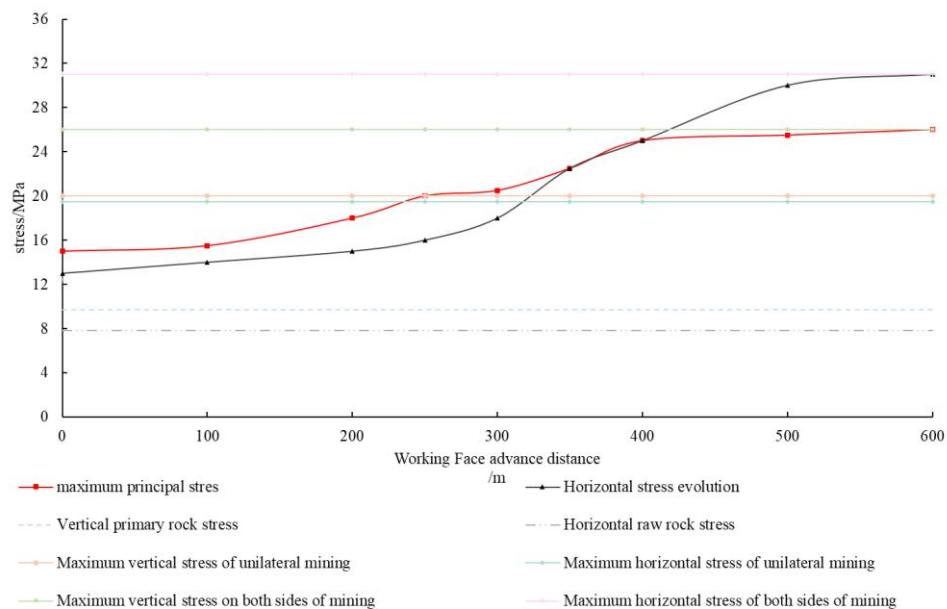

Fig.3.6 Horizontal stress and vertical stress evolution law

Before the working face is advanced to the intersection, the roadway at the measuring station E is affected by engineering disturbance.The vertical stress at both sides of the roadway and the horizontal stress at the roof are greater than the original rock stress, and the vertical stress is greater than the horizontal stress.With the advance of the working face, the vertical stress and horizontal stress of station E are gradually increased under the influence of unilateral mining.After 300m driving to the junction of the working face, the horizontal stress of the main roadway increased significantly due to the impact of bilateral mining,

with an increase greater than that of the vertical stress.As the working surface continues to advance, the horizontal stress eventually exceeds the vertical stress, reaching 30MPa and 25MPa respectively.

To sum up, during the roadway under the influence of tunnelling, unilateral mining and bilateral mining, the increase of horizontal stress at the roof and floor of the roadway was significantly higher than that of vertical stress at the roadway wall, especially the increase of horizontal stress concentration coefficient in the area with intense mining superposition stress to 3.8, while the increase of vertical stress concentration coefficient to 2.6. It can be inferred that the stability of surrounding rock is mainly dominated by horizontal stress.The increase of horizontal stress at the roof of roadway is particularly dramatic after the roadway is affected by mining on both sides.

3.2 Stability study of overburden strata in West Wing Roadway

3.2.1 Analysis of "key position" of crushed surrounding rock in plastic zone of roadway

The failure law of the surrounding rock of the main roadway with bilateral mining can be described from the expansion law of the plastic zone under the influence of the main roadway with unilateral mining and the influence of bilateral mining. FIG. 3.7 shows the plastic zone distribution of the roadway surrounding rocks under unilateral mining stress only.
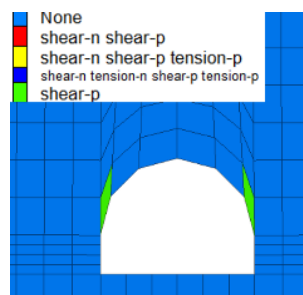

Fig.3.7 Surrounding rock failure law

It can be seen from the figure that when the roadway surrounding rock is subjected to unilateral mining, only the plastic zone appears at the bottom Angle on both sides of the roof. Under the influence of mining stress, the plastic zone

of surrounding rock is small, but it can be seen that the plastic zone initially appears at two corners of roadway roof.
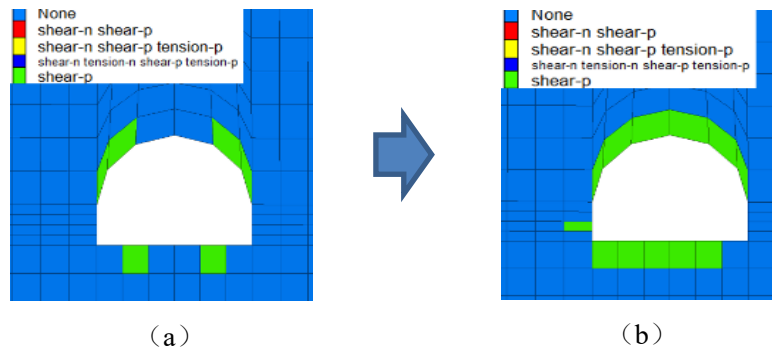

（a）　　　　　　　　　　　　　　　　　　（b）

Fig. 3.8 Distribution of plastic zone under the influence of bilateral mining

With the continuous advance of working faces on both sides of the roadway, when the roadway is affected by mining, the plastic zone at the two corners of the roof begins to gradually expand, as shown in Figure 3.8 (a). At this time, part of the plastic zone also appears in the middle of the roadway floor. The plastic zone of roadway roof extends from a small area affecting only two corners of roadway roof to a large area affecting both sides of roadway roof. As the working face continues to advance, the plastic zone of roadway roof continues to expand until all the upper strata of roadway roof are destroyed. At this time, the plastic zone of the roadway floor also expands, and part of the plastic zone appears on one side of the roadway, but the influence range is small, as shown in Figure 3.8 (b).

Because the distribution of aluminous mudstone soft interlayer within 0-3m of roadway roof strata is not taken into account in the numerical simulation, the plastic zone of the roof in practice will be larger than that in the simulation. The numerical simulation experiment can obtain the development trend law of the plastic zone of roadway roof. The plastic zone of roadway roof extends along the staggered expansion axis of the two working faces, from the initial two angles of roadway roof to all the roadway roof. Therefore, the 45° on both sides of the roof of the roadway is the "key position" of crushed surrounding rock in the plastic zone of the roadway. However, how to prevent the plastic zone from appearing only at the two corners of the roadway roof and finally extending to all the roadway

roof will be the key to control the stability of the overlying strata in the West wing roadway.

3.2.2 "Key location" analysis of the regional location of mining stress in the roadway

①Analysis of plastic zone of roof

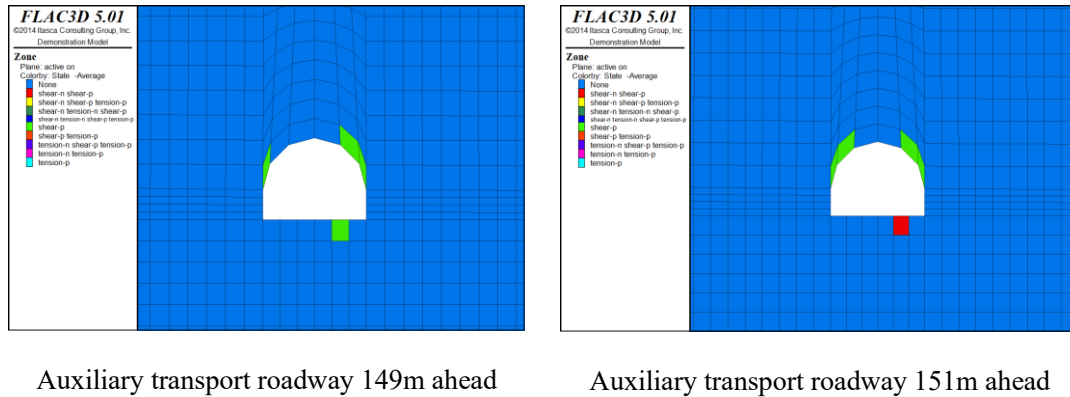Auxiliary transport roadway 149m ahead   Auxiliary transport roadway 151m ahead

Fig. 3.9 Roof plastic zone range of auxiliary transportation roadway

At the auxiliary transport roadway 149m ahead of the No.50114 working face, the width of the plastic zone in the upper left corner of the roof is 1.5m. However, at 151m ahead of the No.50114 working face, the plastic zone in the upper left corner of the roof extends. Therefore, the leading influence range of the roof of auxiliary transportation roadway is 150m.

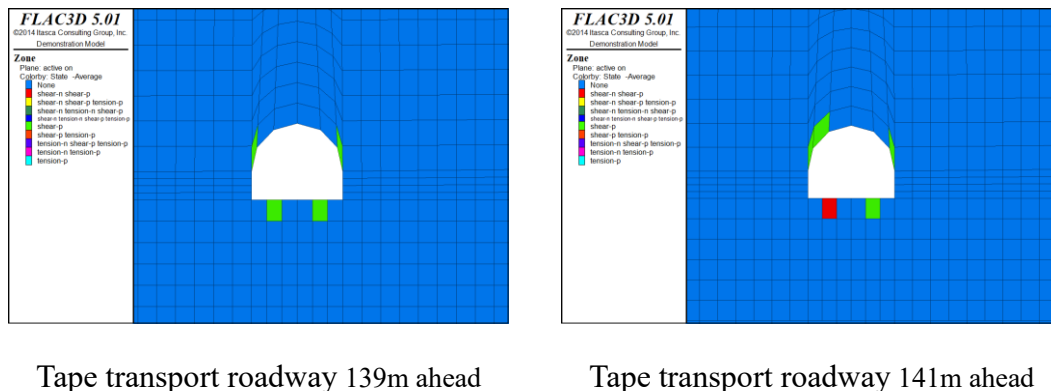Tape transport roadway 139m ahead   Tape transport roadway 141m ahead

Fig. 3.10 Scope of plastic zone of roof of rubber conveying roadway

At the tape transport roadway 1m behind of the No.50201 working face, the width of the plastic zone in the upper left corner of the roof is 1.5m. At 1m ahead of the No.50201 working face, the plastic zone in the upper left corner of the roof is 0.5m

wide. Therefore, the hysteresis influence range of the roof of the tape transport roadway is 140m.
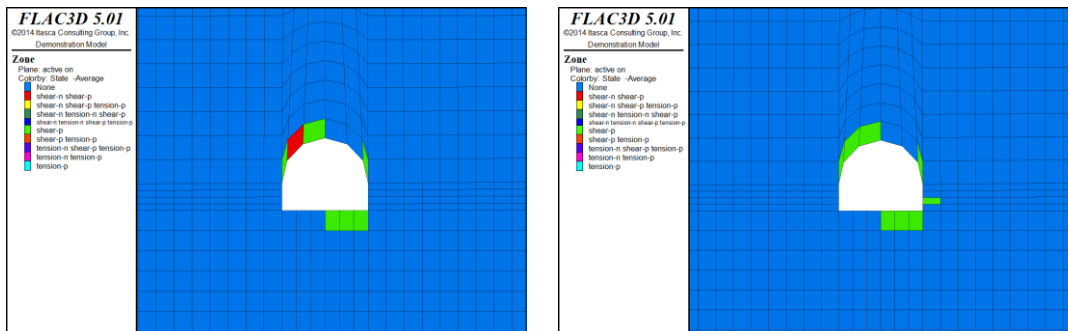
②Analysis of the range of plastic zone of roadway side
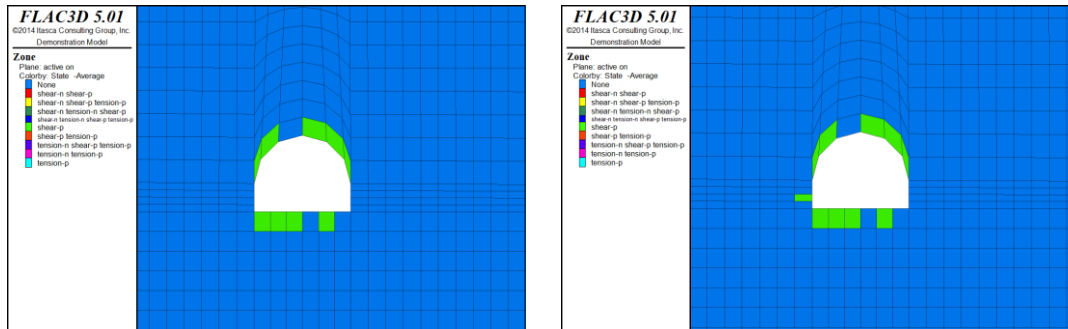
| Auxiliary transport roadway 89m behind | Auxiliary transport roadway 91m behind |

Fig. 3.11 Scope of plastic zone of auxiliary transportation roadway

There is no plastic zone on the left side of the roadway at 89m behind the No.50114 working face. At 91m behind the No.50114 working face, the plastic zone width on the left side of the roadway is 0.4m.Therefore, the hysteresis influence range of the roadway side of auxiliary transportation is 90m.

| Tape transport roadway 169m behind | Tape transport roadway 171m behind |

Fig. 3.12 Scope of plastic zone on the roadway side of the rubber transport roadway

There is no plastic zone on the right side of the roadway at 169m behind the No.50201 working face. At 171m behind the No.50201 working face of tape transport Roadway, the plastic zone width on the right side of roadway is 0.4m.Therefore, the hysteresis influence range of tape transpor roadway is 170m.
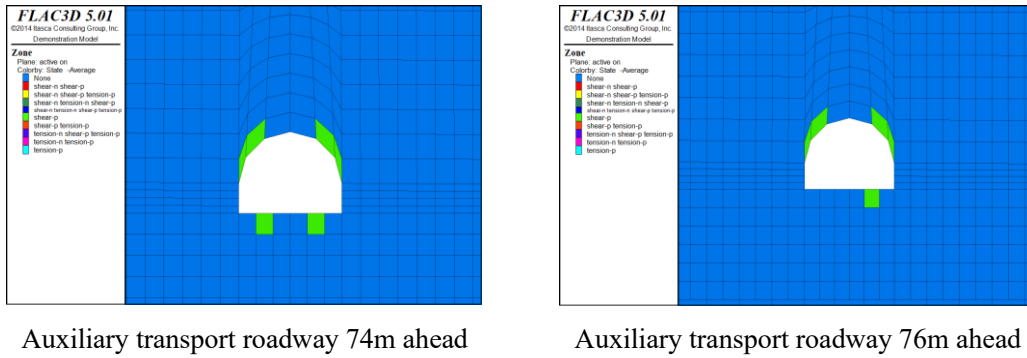
③Analysis of plastic zone of floor plate

Auxiliary transport roadway 74m ahead   Auxiliary transport roadway 76m ahead

Fig. 3.13 Scope of floor plastic zone of auxiliary roadway

In the auxiliary transport roadway, 76m in front of the No.50114 working face, there is no plastic zone at the left bottom Angle of the roadway. At 74m in front of the No.50114 working face, the plastic zone width of the left bottom corner of the roadway is 0.9m. Therefore, the hysteresis influence range of auxiliary transportation roadway is 75m.

Tape transport roadway 69m ahead   Tape transport roadway 71m ahead

Fig. 3.14 Scope of plastic zone of rubber conveyor roadway floor

There is no plastic zone at right bottom Angle of roadway floor at 71m in front of No.50201 working face. At 69m in front of the No.50201 working face,the plastic zone width of the right bottom Angle of the roadway is 0.9m.Therefore, the lead influence range of tape transport roadway is 70m.

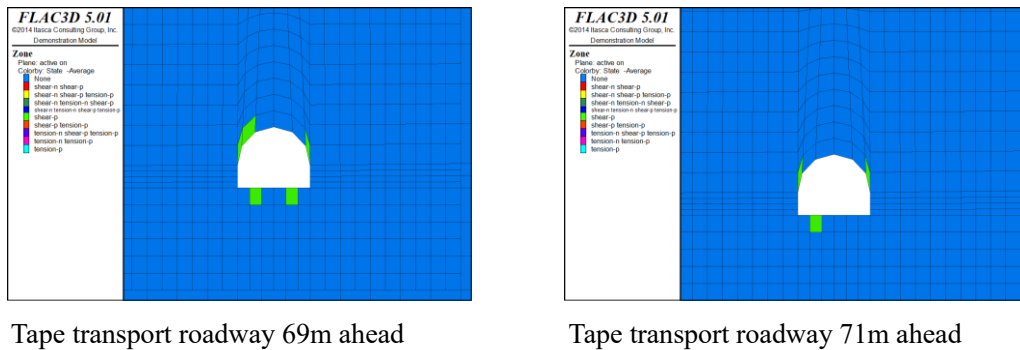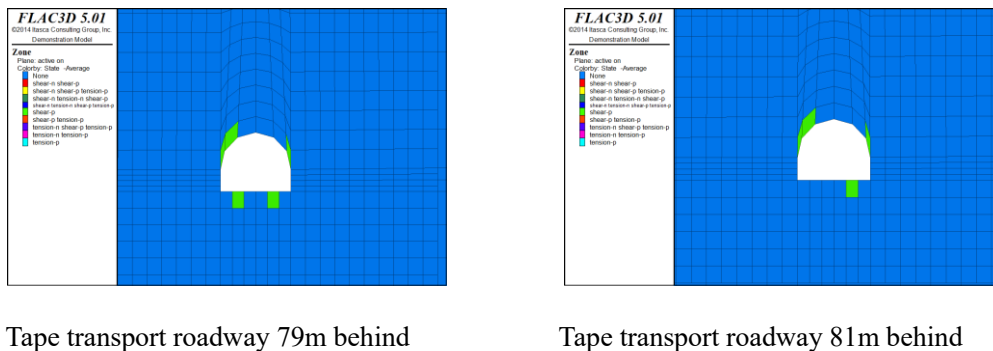Tape transport roadway 79m behind   Tape transport roadway 81m behind

Fig. 3.15 Scope of plastic zone of rubber conveyor roadway floor

There is no plastic zone at left bottom Angle of roadway floor at 81m behind No.50201 working face.However, the plastic zone width of the left bottom Angle of the roadway is 0.9m at the 79m behind the No.50201 working face. Therefore, when the working face is pushed to 450m at the intersection, the lag influence range of the roadway side of the tape transport roadway is 80m.

Due to the large size of the model, the cell size of the plastic zone meshing area is equal to 0.5m of the actual size. According to the development law of the plastic zone, it can be inferred that when the grid is dense enough, part of the plastic zone will occur around the roadway under the influence of mining, but the plastic zone will still expand to other parts from two angles of the roof and floor.

From the above rules, it can be found that the plastic zone of surrounding rock begins to expand when the roadway is simultaneously affected by mining stress of working faces on both sides. The extension part starts from the top Angle on both sides and eventually gradually extends to all the positions of the roadway roof. The position where the plastic zone begins to expand can be obtained through simulation analysis. The plastic zone extension range can be made into the following table by studying the plastic zone extension range.

Tab. 3.1 Influence of plastic zone on the location of two side mining roadway

Advance distance /m		Auxiliary transport roadway		Tape transport roadway	
		Advance range of influence /m	Hysteresis range /m	Advance range of influence /m	Hysteresis range /m
0	roof	40	-	5	15
	floor	-	-	-	-
150	roof	35	-	20	25
	floor	-	60	-	90
250	roof	30	-	60	25
	floor	-	85	-	125
300	roof	130	215	140-	115
	floor	-	60	-	95
450	roof	150	55	135-	120
	floor	75	50	70	80
600	roof	140-	170	120	155
	floor	70	20	-	30

It can be seen from table 3.1 above that the influence range of both sides of mining movement. When the working faces meet, the leading influence range of the auxiliary roadway roof is 150m in front of the 50114 working face, and the lagging influence range is 170m behind the 50114 working face. Glue transported roadways lag effect in the range of 50201 working face roof rear 5 m. auxiliary transport roadways of lag effect in the range of 50114 working face of two rear 90 m. glue transported roadways of lag effect in the range of 50201 working face of two rear 80 m. Auxiliary transport roadways rear backplane lag effect in the range of 50114 face 20 to 50 m. Glue transported roadways rear backplane lag effect in the range of 50201 face 30-80 m. Therefore, the "key location" of the area with a severe influence of mining stress in the roadway is 150m ahead and 150m behind at the junction of the two working faces.

4 Key control technology and scheme for surrounding rock of double - sided mining roadway

4.1 The control idea of surrounding rock of double - sided mining roadway

Produce plastic surrounding rock, the plastic zone of broken rock, to a certain extent, deformation of the elastic zone of surrounding rock, can increase the surrounding rock elastic-plastic interface the minimum principal stress and reduce the maximum principal stress, the inhibition of roadway surrounding rock plastic zone boundary extension, so maintain the stability of the plastic zone fracture rock, can improve the stress state of the plastic zone of surrounding rock, conducive to the stability of surrounding rock of roadway.

The deformation and failure of surrounding rock is actually caused by the formation and development of the plastic zone of surrounding rock. Bilateral mining roadway surrounding rock control is the key to prevent malignant expansion of surrounding rock mass, because of the support resistance cannot from engineering measure to decrease the size of plastic zone of surrounding rock, so to prevent the vicious expanding of surrounding rock mass is the key to maintain the stability of the plastic zone rupture rock mass and avoid the rupture of the plastic zone of surrounding rock instability caused deterioration of surrounding rock stress state.

Through the above analysis, mainly of plastic zone of surrounding rock of roadway influenced by mining stress field control, broken surrounding rock stability have promoting effect to prevent the vicious expanding of the plastic zone, so for mining roadway surrounding rock on both sides of the core is to improve the control of mining stress effect, reduce the nonuniformity of roadway surrounding rock plastic area, at the same time maintaining the stability of plastic zone and broken rock mass, the inhibition of the plastic zone of surrounding rock from steady to unsteady transformation, prevent vicious expanding of

surrounding rock mass. The main technical approaches to realize the shape control of surrounding rock plastic zone are as follows:

(1) The stress of surrounding rock of roadway is improved to prevent the occurrence of highly uneven plastic zone that is difficult to control

Based on the above research, the initial shape of plastic zone of surrounding rock of roadway is mainly controlled by the mining stress field, the basic is in a state of "mining" given state, with the increase of roadway surrounding rock stress, displacement and plastic zone of roadway surface area increased significantly, especially bilateral superimposed stress field caused by mining, the stress concentration factor can be more than 3 ~ 5 times, through the above research, with 50201 working face in 50114 working face of intersection, roadways affected by mining on both sides, the maximum vertical stress is 25Mpa, which is located at two sides of roadway, the stress concentration factor of 2.6;The maximum horizontal stress is 30MPa, located at the roof and bottom Angle of the roadway, and the stress concentration coefficient is 3.8.

Therefore, mining activities will cause the redistribution of roadway surrounding wrock stress. In order to reduce the influence of roadway surrounding rock stress on roadway deformation and failure, improving the stress state of roadway surrounding rock plays an important role in the stability of roadway surrounding rock.

Roadway surrounding rock stress way to improve is the essence of the human lower roadway stress environment or change the stress state of surrounding rock, reduce the influence of the peak abutment pressure of surrounding rock of roadway is a by optimizing coal seam roadway layout position, mining sequence, the reasonable roadway layout optimization methods such as size of coal pillar would formation of the low stress area after mining, the second is artificially in roadway surrounding rock for drilling, loose blasting, slitting, slitting, technical measures, such as digging guide lane to form certain depth of roadway surrounding rock weakening zone, transferring the stress of the surrounding rock of shallow clusters to the depths.

(2) To improve the strength of crushed surrounding rocks in the plastic zone of roadway and prevent the malignant expansion of the boundary of the plastic zone

Two measures can be taken to improve the strength of the fractured surrounding rocks in the plastic zone of the roadway. First, the grouting of the fractured surrounding rocks can fill the cracks in the surrounding rocks, consolidate the fractured rock mass, improve the strength of the surrounding rocks in the plastic zone, and promote the stability of the boundary of the plastic zone. On the other hand, reasonable support technology can prevent the instability of crushed surrounding rock in plastic zone.

In the roadway surrounding rock stress control and grouting to enhance the strength of the surrounding rock more abundant research results, in the engineering practice has also achieved good results, but there are also large quantities of engineering, high cost problems, under certain circumstances to be considered.

4.2 The "space trinity" key control technology for the stability of the surrounding rock of the two-side mining roadway

On grass ditch ore is currently supporting technology, supporting form mainly adopts roadways normal to anchor rod (rope) supplemented, grouting reinforcement supporting system, the early grass ditch coal mine west wing three roadways by the supporting system, according to the in-situ observation, the slag concrete roof only partial existed, as shown in figure 4.1, but the roadways surrounding rock stress field in the current environment basic remain stable, so do not use large quantities of the first technique way of drilling, cutting and unloading method to change the stress state of surrounding rock of roadway.

Fig. 4.1 Picture of concrete slagging in the roof of the roadway

As the two working faces continue to advance, it is bound to cause the superposition of mining stress on both sides before and after the intersection. In particular, the roof surrounding rock of the roadway will continue to be severely damaged, which may cause a large area of concrete to drop slag and injure people, hindering the pedestrians in the roadway. More severe cases may result in roof caving. It is the key to control the stability of roadway surrounding rock in the area with severe superposition stress. Therefore, based on the above research results, this project proposes a key control technology system with the trinity of "key strata + key position + key location" space, as shown in Figure 4.2.The three key location on the system from the space into a whole constitute the combined support system, this system can improve the roadways weak unstable compound roof strata of the bearing capacity of the "key strata", inhibit roadways crushed surrounding rock of the plastic zone "key positions" malignant expansion, guarantee the mining stress drastically affected area position "key location" the stability of surrounding rock, so as to effectively prevent slag concrete bedding face off cuts, reduce the maintenance cost roadways, guarantee the roadways road pedestrian smoothly.
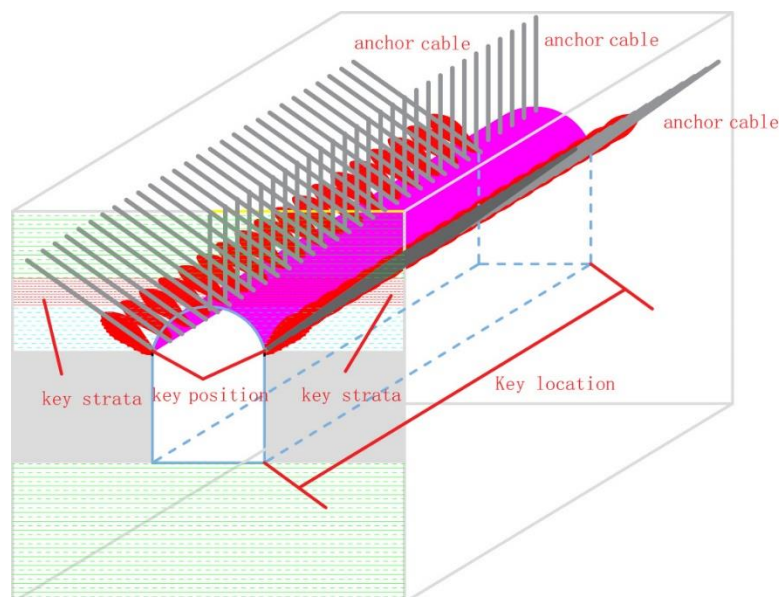

Fig. 4.2 Schematic diagram of "spatial trinity" key control technology system of roadway surrounding rock

4.3 Test roadway surrounding rock control scheme

When roadways surrounding rock deformation is small, the key position and horizon of bolts and cables, inhibit roadways crushed surrounding rock of the plastic zone of malignant expansion, to improve the overall roadways of the bearing capacity, cracks in the roadways in advance local area roof hanging net + ladder beam reinforcing roof bolting, prevent fall from broken concrete, concrete supporting parameters as shown in figure 4.3.When the local section of the surrounding rock of the roadway is deformed and destroyed greatly, after the roof and floor of the belt roadway and the auxiliary roadway are destroyed to a certain extent, the local grouting reinforcement method is adopted, which has a better effect. Considering that there is no traffic or coal transport in the return air roadway, the two sides and the bottom slab are expanded and undercover, and the roof slab can also be partially reinforced by grouting.
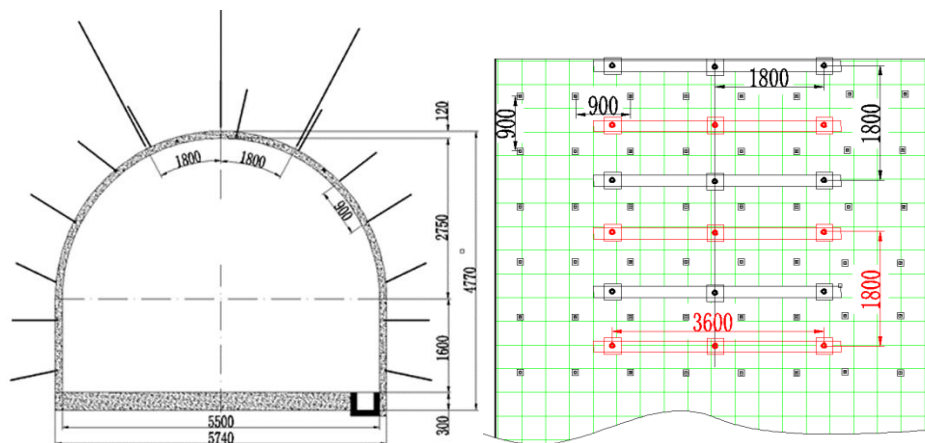
Fig. 4.3 Section and plan of west wing roadway control plan

Based on the observation of ore pressure, it can be seen that within 200 days from the observation of the surface of the two sides of the three large roadways in the west wing of Hecaogou Mine, the overall moving amount of the two sides of the three tunnels does not exceed 15mm, the roof is basically without deformation, and only partial concrete slag dropping phenomenon exists in the roof. However, as the two working faces continue to advance, it is bound to cause the superposition of mining stress on both sides before and after the intersection. In particular, the roof surrounding rock of the roadway will continue to be severely

damaged, which may cause a large area of concrete slag dropping and hurt people, hinder the pedestrians in the roadway, and more seriously, may lead to roof caving accident. Therefore, net hanging + roof anchor cable + ladder beam reinforcement support is adopted. The design of support parameters is as follows:

The original support scheme: 20 mm in diameter, length 2400 mm sinistral without longitudinal reinforcement Ⅱ level without longitudinal ribbed rebar anchor, between row spacing is 900 x 900 mm, plate specifications for 150 mm * 150 mm * 12 mm steel plate, metal type resin cartridge adopts MSCK28/35, each bolt use 3 volume ;Φ 6.5 mm diameter, mesh grid 100 x 100 mm, specifications for 2400 x 1000 mm, reinforcement fabric lap 100 mm, with 14 # twin wire for symmetric binding, binding spacing is not more than 300 mm; Anchor rope Φ 17.8 mm * 7900 mm, the plate is 300 mm x 300 mm x 16 mm, each anchor cable used 5 root MSCK28/35 resin cartridge, prestress is not less than 140KN (36 MPa);Adopt 18 round steel (4000×150mm) ladder beam, 3-3 arrangement, row spacing between anchor cables 2000×2000mm.

And 50114 working face of 50201 face interchange, affected by the superposition of bilateral mining, considering the roadways weak unstable compound roof strata "key strata" 0 ~ 3 m range, due to the bolt length is less than the key strata, so choose to adopt the grass ditch of mine for anchor cable Φ 17.8 mm x 7900 mm control key "horizon", improve the roadways weak composite roof range 0 ~ 3 m "key strata" unstable strata bearing capacity; Considering the 45 degree Angle on both sides of the roof of the fractured surrounding rock in the plastic zone of a large roadway, 1 anchor cable was added at each of the two roof angles of the roadway in advance to inhibit the malignant expansion of the fractured surrounding rock in the plastic zone of the two roof angles of a large roadway. For the area of "key location" where mining stress has a severe impact on the location of the roadway, the area 150m ahead and 150m behind at the intersection of the two working faces, 300m concentrated regional roof was selected for net hanging + anchor cable + ladder beam support. Specific parameters:Roadways roof Φ 17.8 mm x 7900 mm of anchor cable 3 root, root 2 layout at the top of the roadways two 45 Angle, 1 root layout're couple and row spacing between anchor cable is 1800 x 1800 mm, plate of 300 mm x 300 mm x

16 mm, each anchor cable used 5 root MSCK28/35 resin cartridge, 18 round steel ladder beam using phi (4000 x 150 mm), 3-3 to decorate, Φ 6.5 mm diameter, mesh grid 100 x 100 mm, specifications for 2400 x 1000 mm, reinforcement fabric lap 100 mm, Use 14# double-ply iron wire for symmetric binding. The binding spacing should not be greater than 300mm. The position range of the support area is 150m before and after the intersection of the two working faces.

4.4 Test the effect of roadway control

The relative displacement inside two sides and roof of roadway refers to the displacement between multiple points inside surrounding rock. The main purpose of deep base point displacement monitoring is to judge the loose range of surrounding rock and provide a basis for reasonable selection of anchor support parameters.Because the stress of surrounding rock of the roof is transferred and concentrated after the excavation of the roadway, the stratified roof is prone to separation failure after the deformation of the lower rock layer, resulting in potential accidents. The displacement observation of surrounding rock of different depths of the roof can grasp the situation of the separation failure area, etc.The displacement observation of surrounding rock at different depths of the two sides can master the change, formation process and morphological characteristics of the loose circle of surrounding rock at different depths of the two sides, understand the plastic zone distribution of the two sides of coal, judge the support effect, and obtain the basic field data for the optimization of bolt (cable) length parameters and the determination of reasonable bolt length and stress analysis [65].

4.4.1 Deep base point displacement observation scheme

Two basis points digital depth basis point displacement meter was used for the observation of roadway displacement, 1.0m and 2.5m two basis points were used for the two sides, and 1m, 2.5m, 4m and 8.0m two basis points were used for the roof to form four basis points. The observation instrument and basis points are shown in Figure 4.5.By observing the relative displacement of surrounding rock at different depths and at different times, the deformation of surrounding rock at

different depths of the roadway can be reflected, and the separation of rock strata at different depths of the roadway can be understood.
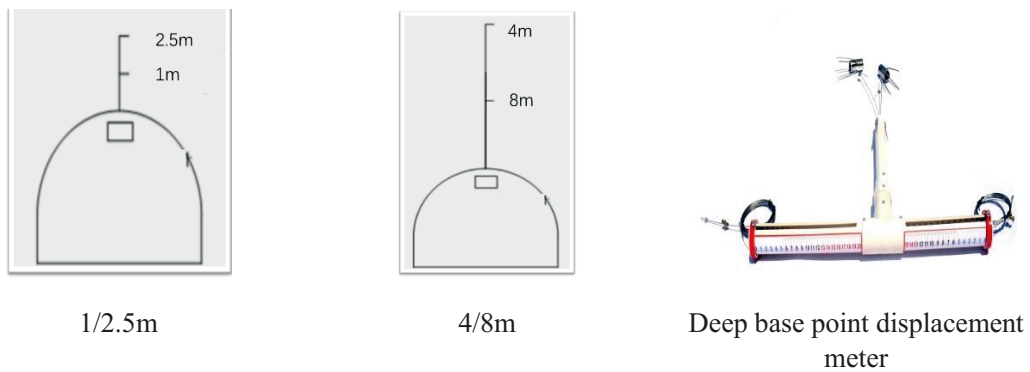

| 1/2.5m | 4/8m | Deep base point displacement meter |

FIG. 4.5 Arrangement plan of deep base point displacement meter
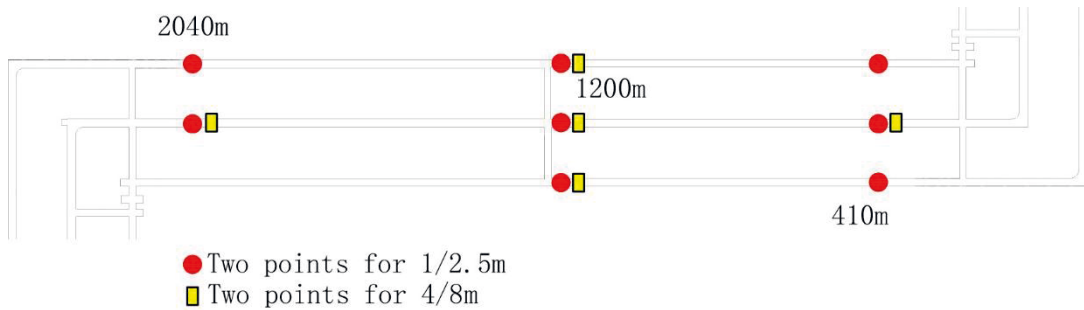

● Two points for 1/2.5m
□ Two points for 4/8m

Fig. 4.6 Location map of deep base point displacement observation station

The deep base point displacement observation was carried out in the Auxiliary canal main lane, adhesive tape main lane and return air main lane in the west wing of Hecaogou Mine. A total of 7 sections of roof were selected for monitoring. The roof holes of each measurement station were located in the middle of the roof and were vertically arranged with a diameter of 28mm, as shown in Figure 4.6.

4.4.2 data processing and analysis

By monitoring these observation points, the value of each deep base point displacements meter is continuously recorded over a period of 200 days. From February 20, records were made every 15-20 days, and 12 roof separation data were recorded in 200 days. This study focuses on the stress change and surrounding rock stability before and after the intersection of two mining roadway. Therefore, the strata separation at 1200m of Auxiliary roadway and tape transport roadway is taken as the research object. The observation data of deep base point displacement are as follows.

（1）Observation of deep base point of main roadway in West Wing Auxiliary Transportation

Observation of roof separation of The Main roadway of West Wing Auxiliary Transport system has been carried out since February 20. The observation data of deep base point of the roadway are shown in Table 4.1.

Tab. 4.1 Displacement of deep base point of auxiliary transportation roadway

data	displacement /mm			
	0-1m	0-2.5m	0-4m	0-8m
2.20	0	0	0	0
3.10	0	1	1	1
3.28	0	1	1	1
4.14	1	2	2	2
5.3	2	3	3	3
5.19	3	4	5	5
6.2	3	5	6	6
6.21	4	9	11	12
7.5	5	11	13	14
7.18	5	12	14	15
8.2	5	12	14	15
8.19	5	12	14	15

After statistical analysis of the data of the main roadway of the West Wing Auxiliary Transportation, it is found that the displacement meter of the roof depth base point before 7.18 gradually increases, and the displacement at 0-1m reaches the maximum 5mm, 0-2.5m 12mm, 0-4m 14mm, and 0-8m 15mm.According to the above data, draw it into a line graph as shown in the figure below.
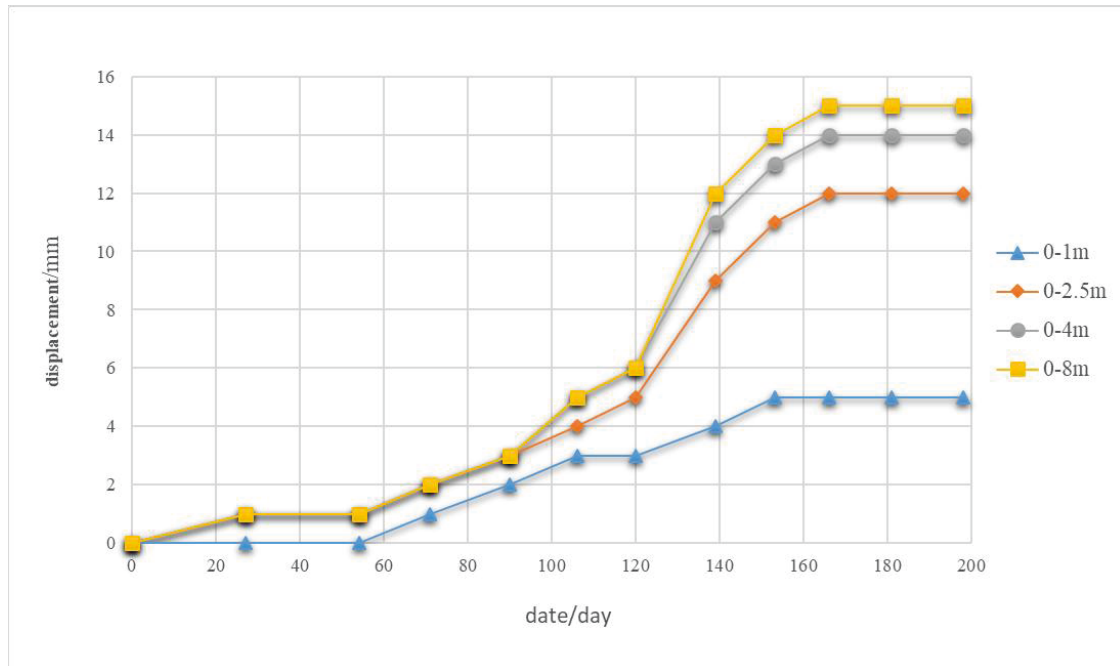
Fig. 4.7 Displacement observation diagram of two deep base points at 1200m of auxiliary transportation roadway

As can be seen from the figure, the displacement of the roof increased significantly at 110 days, which was caused by the advance of working faces on both sides to the same position at this time, which increased the displacement of the roof. However, the separation of the roof gradually stabilized after 160 days.It can also be seen from the figure that the roof separation is mainly concentrated in the upper surrounding rock of the roadway within the range of 2.5m, and the roof separation reaches 12mm within the range of 2.5m, which is basically consistent with the range of roof unstable rock obtained in the study on the stability of surrounding rock of the roadway. In addition, according to the trend shown in the figure, the roadway roof separation tends to be stable after 160 days, and the amount of roadway roof separation is within the acceptable range, indicating that the roadway roof is effectively controlled and the proposed roadway surrounding rock stability control technology is effective and feasible.

（2）Observation of the deep base point of tape transport roadway

The observation of roof separation in The West Wing Jiao-yun roadway began on February 20, and the observation data of its deep base point are shown in Table 4.2.

Tab. 4.2 Displacement of deep base point in return air roadway

date	displacement /mm			
	0-1m	0-2.5m	0-4m	0-8m
2.20	0	0	0	0
3.10	0	0	0	0
3.28	1	1	1	1
4.14	1	2	2	2
5.3	1	2	2	2
5.19	1	2	2	2
6.2	2	4	5	5
6.21	2	4	6	7
7.5	3	7	9	10
7.18	3	8	10	11
8.2	3	8	10	11
8.19	3	8	10	11

After statistical analysis of the data of The West Wing Jiao-yun roadway, it is found that the value of the displacement meter of roof depth base point before 7.18 gradually increases, and the displacement reaches the maximum 3mm at 0-1m, 8mm at 0-2.5m, 10mm at 0-4m, and 11mm at 0-8m.According to the above data, draw it into a line graph as shown in the figure below.
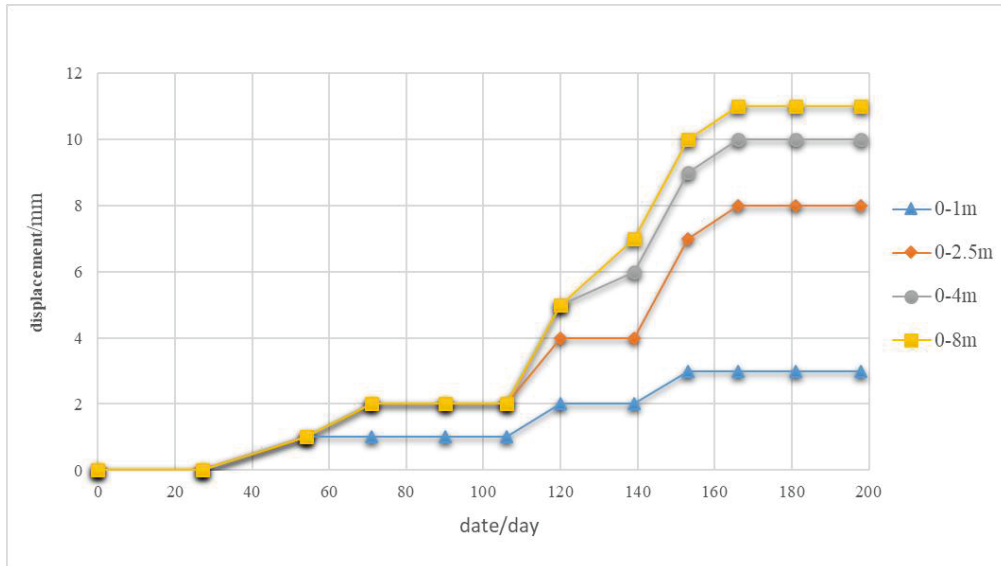

Fig. 4.8 Displacement observation chart of two deep base points at 1200m of tape transport roadway

As can be seen from the figure, the displacement of the roof increased significantly at 120 days, which was caused by the advance of working faces on

both sides to the same position at this time, which increased the displacement of the roof. However, the separation of the roof gradually stabilized after 150 days.It can also be seen from the figure that the roof separation is mainly concentrated in the upper surrounding rock of the roadway within the range of 2.5m, and the roof separation reaches 8mm within the range of 2.5m, which is basically consistent with the range of roof unstable rock obtained in the study on the stability of surrounding rock of the roadway.Moreover, according to the trend shown in the figure, the roadway roof separation tends to be stable after the 150th day, and the amount of roadway roof separation is within the acceptable range, indicating that the roadway roof is effectively controlled and the proposed roadway surrounding rock stability control technology is effective and feasible.

Figure 4.9 for 50201 face and roadways of the surrounding rock control after 50114 working face of intersection diagrams, can be seen from the graph, basic no roadways surrounding rock deformation, nor concrete shotcrete layer peeling, until the work is picking, three roadways basically stable, the control effect is good, effectively prevent the slag concrete bedding face off cuts, reduced the maintenance costs of roadways, guarantee the safe and efficient mining.

Fig. 4.9 Control effect diagram of roadway surrounding rock

5 Main Conclusions

This research has completed all the research content, has achieved the research objective, and has made certain scientific research achievements. In the research process of this project, the geomechanical detection of surrounding rocks of double-side mining roadway in Hecaogou Coal Mine was studied by combining field investigation, field measurement, laboratory experiment, numerical simulation and theoretical analysis and field engineering practice.At the same time, the evaluation factors of the stability of the two sides of the roadway and the evolution law and superposition effect of the mining stress field on the two sides of the mining face are put forward.The failure mechanism and plastic zone expansion law of the surrounding rock of two sides mined-out roadway are also obtained, and the key control technology and scheme for the stability of two sides mined-out roadway surrounding rock are put forward.The main conclusions are as follows:

1. Stability of surrounding rock strata in the double sides of mining roadway:

(1) based on the horizontal analysis of borehole peeping results at the three measuring points of the roof of the west wing return wind roadway, the thickness of the low oil shale of the roadway roof ranges from 3.0 to 5.10m within the range of 410m to 2240m, and the thickness of the argillaceous siltstone adjacent to the oil shale ranges from 3.4 to 6.90m.Within the range of 410m~1240m, the overall thickness of oil shale increases slightly, from 3.6m to 5.10m.The overall thickness of argillaceous siltstone increased significantly from 3.4m to 7.90m.Within the range of 1240m~2240m, the overall thickness of oil shale decreases significantly from 5.10m to 3.0m.The overall thickness of argillaceous siltstone decreases greatly from 7.90m to 3.85m.Within 0-3m of the roof of the roadway, the oil shale has the rich area of aluminum-earth mudstone rock line, the rich area of aluminum-earth mudstone extremely thin layer of 1-2cm, the rich area of aluminum-earth mudstone thin layer of 5-10cm and the rich area of "belly meat" of the interlayer of aluminum-earth mudstone and oil shale.The rich area of oil shale with aluminum-earth mudstone is mainly in the range of 1.2-1.8m above the roof.Aluminium-earth mudstone 1~2cm extremely thin rock rich area is mainly concentrated in the range of 0 ~ 1.1m above the roof.The 5~10cm thin layer rich area of aluminous mudstone mainly concentrates in the range of 0-2m above the roof, and the height from 410m

to 1240m to 2240m from the roof layer decreases gradually.The "belly flesh" rich area of the interbedded aluminum-earth mudstone and oil shale is mainly in the range of 2-3m above the roof.

(2) After the systematic analysis of the borehole peeping results, the specific distribution horizon of the aluminum mudstone soft interlayer was determined, and the roof strata columnar diagram containing the aluminum mudstone soft interlayer was depicted.The distribution law of soft intercalation of aluminaceous mudstone in the whole roadway under ideal conditions is established. It is determined that 0-3m of the roadway roof is an unstable rock layer, and targeted support is needed.

2. Study on evolution law and superposition effect of mining stress field on both sides of stoping face:

(1) According to the law of vertical stress concentration, when the west wing roadway is not disturbed by engineering, the vertical stress is 9.7mpa;During tunneling, the maximum vertical stress around the roadway was 15MPa, 1.5 times that of the original rock. Before the intersection of 50114 working face and 50201 working face, during the period when the roadway was only affected by unilateral mining, the maximum vertical stress around the roadway is 20MPa and located at the two sides of the roadway. The stress concentration coefficient is 2.1, 1.3 times that of the excavation period. After the intersection of 50114 working face and 50201 working face, the roadway was affected by bilateral mining. The maximum vertical stress around the roadway increased to 25MPa compared with that of unilateral mining, and was located at both sides of the roadway. The stress concentration coefficient was 2.6, which is 1.7 times that of the excavation.

(2) According to the law of horizontal stress concentration, the horizontal stress of the West Wing roadway is 7.8mpa without engineering disturbance.The maximum horizontal stress is 13MPa, which is 1.7 times of the original rock stress.Before the intersection of 50114 working face and 50201 working face, the roadway was only affected by unilateral mining. The maximum horizontal stress around the roadway was 20MPa, and it was located at the roof and bottom Angle of the roadway. The stress concentration coefficient was 2.5, 1.5 times that of the excavation period.After the intersection of 50114 working face and 50201 working face, the roadway is affected by bilateral mining. The maximum horizontal stress around the roadway is

30MPa and located at the roof and bottom Angle of the roadway. The stress concentration coefficient was 3.8, which is 2.3 times that of the tunneling period.

3. Evolution law and key position and location stability of surrounding rock plastic zone of bilateral mining-induced roadway:

(1) From the evolution law of the plastic zone, it can be seen that the expansion of the plastic zone of the two sides of the mining roadway begins at the two corners of the roadway roof. With the influence of mining, the plastic zone at the two corners of the roadway roof gradually expands to the middle of the roadway roof until it is all covered.Therefore, the two corners of the roof are the "key position" to prevent the malignant expansion of the plastic zone.

(2) From the influence range of mining on both sides, it can be seen that after the working faces meet, the leading influence range of the roof of auxiliary roadway is 150m in front of the 50114 working face, and the lagging influence range is 170m behind the 50114 working face.The lagging influence range of the two sides of the Auxiliary transport roadway is 90m behind the working face, and that of the two sides of the Jiaoyun roadway is 80m behind the working face.The lagging influence range of auxiliary roadway floor is 20-50m behind the working face of 50114, and 30-80m behind the working face of 50201.Return air roadway has little effect.With the advance of the working face, this distance fluctuates within a certain range, but does not change dramatically. Therefore, it can be speculated that the influence range of the plastic zone of roadway roof affected by bilateral mining is 150m ahead working face and 150m behind working face, which is the "key location" to control the malignant expansion of the plastic zone.

4. Key control technologies and schemes for the stability of surrounding rocks of two-way mining-induced roadway:

(1) put forward "the key strata + key position +key location" space of the trinity system of key control technology, the system from the space on the three key position combined into a whole constitutes the combined support system, this system can improve the alleys weak unstable compound roof strata of the bearing capacity of the "key strata ", inhibit alleys crushed surrounding rock of the plastic zone "key positions" vicious expanding, guarantee the mining stress drastically affected regional location "key location" the stability of surrounding rock.

(2) Based on the deformation and failure characteristics of the roadway at different mining influence stages obtained through whole-course tracking observation, the supporting scheme of the roadway surrounding rocks under such deformation and failure characteristics is proposed, which is as follows:

Bolt and anchor cable should be provided at key positions and layers to inhibit the malignant expansion of crushed surrounding rocks in the plastic zone of the roadway and improve the overall bearing capacity of the roadway. In advance, net hanging + roof anchor cable + ladder beam reinforcement support should be carried out in the local area of the cracked roof of the roadway to prevent the broken concrete from falling down and injuring people.Superimposed stress before alleys intersection the area controlled by the alleys of roof rock mass damage, supports the plan to "hang net + ladder beam" is given priority to get the better control effect, This effectively prevents the slags of roadway slag concrete, reduces the maintenance cost of roadway, and ensures safe and efficient mining of roadway.

6 Reference

1. Wang lujun, Zhou hongwei, Rong tenglong, et al. Evolution law and disturbance characteristics of mining stress field in deep coal [J]. Journal of rock mechanics and engineering,2019,38(S1):2944-2954.

2. Shengwei Li,Mingzhong Gao. Numerical simulation of spatial distributions of mining-induced stress and fracture fields for three coal mining layouts[J]. Elsevier B.V.,2018.

3. Zhang Shujing. Research on the relationship between rock burst pressure and mining stress Field of shallow coal seam working face [J]. Coal Mining,2018, 23(03):79-82+55.

4. Sun Yue. Evolution law of mining stress field and experimental study on overburden failure Pattern [D]. Hebei University of Engineering,2018

5. Zhou ping, Jiang junjun, Lin leibin, et al. Analysis on large deformation and mining stress field of stoping roadway in extra-thick coal seam [J]. Coal mine safety,2016,47(02):208-211+215.

6. Liu qin-jie, Yang ke, Chen GUI, et al. Study on distribution and evolution characteristics of mining stress in fully mechanized coal caving face based on measured in-situ stress [J]. Journal of mining and safety engineering, 2016, 33(01):109-115.

7. Wang hongwei, Jiang yaodong, Yang tian, et al. Study on distribution characteristics of mining stress field under fault structure occurrence [J]. Coal engineering,2016,48(01):92-94+98.

8. Jiang pengfei, Dai shengfu,Liu jinrong, et al. Evolution of surrounding rock comprehensive stress field and supporting countermeasures for roadway with strong mining in deep extra-thick coal seam [J]. Coal mining,2015,20(06):60-66.

9. Jianwei Li,Changyou Liu,Tong Zhao. Effects of gully terrain on stress field distribution and ground pressure behavior in shallow seam mining[J]. Elsevier B.V.,2016,26(2).

10. Liu Jie, Wang enyuan, zhao enlai, et al. Experimental study on the distribution of mining stress field in deep working face [J]. Journal of mining and safety engineering,2014,31(01):60-65.

11. Meng Lin Xu,De Shen Zhao. Analysis of Three-Dimensional Numerical Simulationin on Overlying Strata's Stress Field and Displacement Field in Thick Seam Mining[J]. Trans Tech Publications Ltd,2013,2438.

12. Zhao qi-feng, Wang yu-huai, Meng xiang-rui, et al. Numerical simulation study on mining stress field and deformation and failure characteristics of coal seam floor [J]. Mining research and development,2009,29(02):25-27.

13. Wang zhen, Hu qianting, Wen guangcai, et al. Distribution characteristics of mining stress field and analysis of its control effect on coal and rock gas dynamic disaster [J]. Acta coal sinica,2011,36(04):623-627.

14. Zhang penghai, Yang tianhong, Zheng chao, et al. Rock mass stability analysis based on mining stress field and microseismic activity [J]. Acta coal sinica,2013,38(02):183-188.

15. Gao mingzhong, Liu junjun, Lin wenming, et al. Study on in-situ stress evolution law of advanced mining in extra-thick coal seams [J]. Coal science and technology,2020,48(02):28-35.

16. Xiaolou Chi,Ke Yang,Qiang Fu,Litong Dou. The Mechanism of Mining-Induced Stress Evolution and Ground Pressure Control at Irregular Working Faces in Inclined Seams[J]. Springer International Publishing,2020,38(1).

17. Sun zhiqiang. Analysis of stress variation law of mining overburden [J]. Energy and environmental protection,2019,41(09):186-189.

18. Daniel Pawelus. Stability Assessment of Headings Situated in a Field of High Horizontal Stress in Polish Copper Mines by Means of Numerical Methods[J]. IOP Conference Series: Earth and Environmental Science,2019,221(1).

19. Yuan Fang, MOU Zonglong, Yang Jing, et al. Study on surrounding rock stability of middle roadway in stope face [J]. Coal Mine Safety,2020, 51(02):202-207+212.

20. Liu yongli, Wang zhensuo, Zhang haidong, et al. Study on stability of surrounding rock of roadway roof and overburden sediment outburst law [J]. Coal technology,2019,38(08):1-4.

21. Li xiao-yu, Jiang jin-quan, Ding nan, et al. Stability analysis of surrounding rocks with different roadway section shapes under complex mining conditions [J]. Coal technology,2019,38(07):58-61.

22. Dai changchun, Ma ning, Yang Yang, et al. Study on surrounding rock stability of deep close roadway under the influence of horizontal stress [J]. China coal,2019,45(06):114-119.

23. Zhao zhiqiang, Ma yanjie. Discussion on the stability of roadway surrounding rock and the connotation of butterfly failure theory -- response to "discussion on the butterfly failure theory of roadway and its application prospect >" [J]. Journal of China university of mining and technology, 2019,48(03):685-692.

24. Niu Dezheng. Design of Grouting Fire Prevention and Extinguishing System for Extra Large Mines [J]. Coal Technology, 2017,36(9):165-166.

25. He Fulian, ZHANG Guangchao. Analysis and Control of surrounding Rock stability of deep crushed Soft Rock Roadway [J]. Rock and Soil Mechanics, 2015, 36(05):1397-1406.

26. Zhang zhaoqian, Xu mingde, Liu quansheng. Study on weighted average evaluation method for surrounding rock stability of coal roadway [J]. Rock and soil mechanics, 2009,30(11):3464-3468.

27. Huang qingxiang, Liu yuwei. Limit self-stabilizing equilibrium arch theory of roadway surrounding rock support [J]. Journal of mining and safety engineering, 2014,31(03):354-358.

28. Li weiteng, Li shucai, Xuan chao, et al. Failure mechanism and control of roadway support in high-stress soft rock [J]. Journal of rock mechanics and engineering,2015,34(09):1836-1848.

29. Kang Hongpu. Stress distribution characteristics and Roadway Surrounding Rock Control Technology in deep coal Mines [J]. Coal Science and Technology,2013, 41(09):12-17.

30. Kang hongpu, Wang jinhua, Lin jian. Application case analysis of roadway bolt support in coal mine [J]. Journal of rock mechanics and engineering,2010,29(04):649-664.

31. Kang hongpu. Development of roadway bolt support technology in coal mines in China over the past 60 years and its prospect [J]. Journal of China university of mining and technology, 2016,45(06):1071-1081.

32. Wang Jinhua. Mechanism and Effect Analysis of combined Bolting and cable support in all-coal roadway [J]. Acta Coal Sinica,2012, 37 (01):1-7.

33. Yuan liang, Xue junhua, Liu quansheng, et al. Control theory and support technology of deep rock roadway in coal mine [J]. Acta coal sinica, 2011,36(04):535-543.

34. Kang hongpu, Fan mingjian, Gao fuqiang, et al. Deformation characteristics and support technology of surrounding rock of roadway in over km deep Wells [J]. Journal of rock mechanics and engineering,2015,34(11):2227-2241.

35. Liu hongtao, Wang fei, Wang guanghui, et al. Research on the performance of elongable bolt supporting system for roof of large deformation roadway [J]. Journal of coal industry,2014,39(04):600-607.
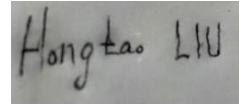
Thesis grade

Thesis: Study on Key Factors of Roadway Roof Stability Control

Author: PengHui Wei

Supervisor: Hongtao Liu   **Grade**: 90   **Signature**:

Co-Supervisor: **Grade**:   **Signature**: